Theoretical Study of the Kinetics of the Hydrogen Abstraction from Methanol. 3. Reaction of Methanol with Hydrogen Atom, Methyl, and Hydroxyl Radicals

Jerzy T. Jodkowski,† Marie-Thérèse Rayez,* and Jean-Claude Rayez

Laboratoire de Physicochimie Moléculaire, CNRS UMR 5803, Université Bordeaux 1, 351, Cours de la Libération, 33405 Talence Cedex, France

Tibor Bérces and Sándor Dóbé

Central Research Institute for Chemistry, Hungarian Academy of Sciences, H-1525 Budapest, P.O. Box, Hungary

Received: November 9, 1998; In Final Form: February 24, 1999

Ab initio calculations at different levels of theory have been performed for the title H-abstraction reactions. Total energies at stationary points of the potential energy surfaces for the reaction systems were obtained at MP2 and MP4 levels and improved by using Gaussian-2 (G2) methodology. The calculated G2 heats of reaction agree well with the experimental ones for both methoxy (product resulting from hydroxyl-side attack) and hydroxymethyl (product resulting from methyl-side attack) reaction channels. Calculations of the potential energy surfaces for the reaction systems show that H-abstraction from methanol by H, CH_3, and OH (for methoxy reaction channel) proceeds by simple metathesis. The mechanism of the hydroxymethyl channel of reaction $CH_3OH + OH$ appears to be more complex, and it may consist of two consecutive processes. The reaction rate is determined by the energy barrier of the first process. Differences in the heights of the calculated energy barriers explain the differences in the reactivity of H, CH_3, and OH toward methanol. The calculated barriers indicate a significant dominance of the hydroxymethyl formation channel for the $CH_3OH + H$ and $CH_3OH + OH$ reaction systems. Rationalization of the derived energy barriers has been made in terms of the polar effect. The calculated rate constants are in very good agreement with experiment and allow a description of the kinetics of the reactions under investigation in a wide temperature range with the precision that is required by practical applications such as modeling of the chemistry of methanol combustion.

1. Introduction

Methanol is one of the simplest oxygenated hydrocarbon compounds. Its combustion produces significantly less air pollutants than that of gasoline. Therefore, methanol may be considered as a promising alternative fuel.[1] As a consequence of the presence of two different types of hydrogen atoms, hydrogen abstraction from methanol yields the isomeric radicals CH_3O and CH_2OH which are characterized by different thermochemistry and reactivity. Recently, reliable results became available for the heats of formation of CH_3O and CH_2OH radicals which indicate that the CH_2OH-forming channel is more exothermic than the CH_3OH-forming reaction by 9.1 kcal/mol.[2] The relative efficiencies of the two product channels may be characterized by the branching ratios. These are of fundamental importance in combustion and atmospheric modeling. Therefore, the reactions of H-abstraction from methanol by atoms and radicals are of interest both from theoretical and from experimental points of view. Elementary reactions of this type have been surveyed in the data compilation of Tsang[3] and in a critical review of Grotheer et al.[4]

The reaction with hydrogen atom plays an important role in methanol combustion. About 53% of methanol consumption is due to the reaction with hydrogen atoms under fuel-rich condition.[4] The kinetics of the $CH_3OH + H$ reaction is not very well-known. Only limited information is available from the study of methanol pyrolysis and direct experiments.[5−9] The results obtained at lower temperature are not in line with the high-temperature expression derived from shock tube measurements.[10] Calculated from Tsang's equation,[3] the overall rate constant is 2.8×10^{-15} cm^3 molecule^{-1} s^{-1}. This value is about 4 orders of magnitude lower than that of the analogous, very exothermic, reaction of methanol with fluorine atoms[11] and about 2 orders of magnitude lower than that of the almost thermoneutral reaction with chlorine.[11,12] This may indicate an important role of the polar effect in the mechanism of the H-abstraction by halogen atoms from methanol. The experimental values of the branching ratio for the reaction channels

$$CH_3OH + H \rightarrow CH_3O + H_2 \quad \text{(R1)}$$

$$\rightarrow CH_2OH + H_2 \quad \text{(R2)}$$

are uncertain and contradictory. On the basis of the thermochemistry (1.2 kcal/mol is the reaction enthalpy for R1 compared with −7.9 kcal/mol for R2, at room temperature), the hydroxymethyl channel is expected to be dominant, but the branching ratio should depend on temperature. A recent theoretical study of Lendvay et al.[13] has revealed that the CH_2OH formation is the dominant reaction channel, contributing to the overall reaction by over 95% below 1200 K and by about 90% at 2000 K.

* To whom correspondence should be adressed.
† Permanent address: Department of Physical Chemistry, Wroclaw University of Medicine, Pl. Nankiera 1, 50-140 Wroclaw, Poland.

10.1021/jp984367q CCC: $18.00
Published on Web 04/24/1999

Both reaction channels were studied experimentally for the reaction of methanol with methyl radical.[3,14]

$$CH_3OH + CH_3 \rightarrow CH_3O + CH_4 \quad (R3)$$

$$\rightarrow CH_2OH + CH_4 \quad (R4)$$

The reaction enthalpies are very close to those for the reaction with hydrogen, i.e., 0.5 kcal/mol and −8.6 kcal/mol for R3 and R4, respectively. The reaction channel which leads to the formation of the hydroxymethyl radical is dominant, but the corresponding branching ratio decreases with a lowering of the temperature.[14] Low-temperature measurements[15] did not find evidence for the occurrence of H-abstraction via channel R3. Results of experiments carried out in solid methanol using the electron spin resonance method show that hydrogen is abstracted mainly via reaction channel R4. A very large isotope effect was observed.[15] At 77 K the H-abstraction from methanol proceeds ca. 1000 times faster than D-abstraction from CD_3OD. An explanation of this, in terms of the quantum tunneling effect, was provided in an ab initio study by Tachikawa et al.[16] The reaction of methanol with methyl radicals proceeds slowly with the overall rate constant[3] of 3.7×10^{-20} cm^3 molecule^{-1} s^{-1} at room temperature, which is about 5 orders of magnitude lower than that for the analogous reaction with hydrogen atoms.[3] The reaction enthalpies for $CH_3OH + CH_3$ and $CH_3OH + H$ are very close for the corresponding reaction channels. This implies considerably higher energy barriers for the reaction of CH_3OH with methyl radicals.

Kinetics of the H-abstraction from methanol by hydroxyl radicals was studied[1c,7,11,17−28] extensively both by experimental and theoretical methods. The greater interest in the OH radical reaction is due to the importance of this reaction in lean and moderately rich methanol flames. A recent flame modeling study of Grotheer et al.[4] predicts that about 38% of methanol consumption is related to the $CH_3OH + OH$ reaction. The detailed direct kinetic measurements in a wide temperature range by Hess and Tully[27] lead to results very close to those recommended by Tsang[3] in his data evaluation regarding the overall rate constant of the $OH + CH_3OH$ reaction. Both reaction channels

$$CH_3OH + OH \rightarrow CH_3O + H_2O \quad (R5)$$

$$\rightarrow CH_2OH + H_2O \quad (R6)$$

are exothermic; the heats of reaction are −13.9 and −23.0 kcal/mol for the R5 and R6 channels, respectively. However, the overall rate constant[3] of 9.1×10^{-13} cm^3 molecule^{-1} s^{-1} is more than that 1 order of magnitude lower than that for the less exothermic reaction of methanol with chlorine.[12] The branching ratio measured at low temperature in several studies[3] is subject to considerable uncertainty. A compromise value of 0.1 seems to be a reasonable estimate for the room-temperature branching ratio of CH_3O formation in the $OH + CH_3OH$ reaction. A definite increase in methoxy yield occurs[11] from the room-temperature value up to a ratio of 0.2−0.3 at 600 K. Hägele et al.[22] reported an even more significant increase.

An explanation of the relative differences in H, CH_3, and OH reactivities toward methanol was a major aim of the present investigation. For the better understanding of the kinetics of the H-abstraction in the $CH_3OH + H$, CH_3, OH reaction systems, we carried out calculations using ab initio molecular orbital theory in order to find the characteristic points of the potential energy surface. Basic properties of these stationary points (reactants, products, transition states, and intermediate complexes) are then used with theoretical reaction rate models to evaluate the rate constants for both reaction channels in a wide temperature range.

2. Molecular Structure Calculations

2.1. Computational Details. Ab intio MO calculations were performed using the Gaussian 92 and 94 packages of computer codes.[29] The geometries of reactants, products, and transition states were first optimized at the restricted Hartree−Fock (RHF) self-consistent field (SCF) level for CH_3OH, H_2, CH_4, and H_2O molecules and at the unrestricted Hartree−Fock (UHF) level for the open-shell species with the 6-31G* and 6-311G** basis sets.[30] The SCF geometries were then refined using the Møller−Plesset many-body perturbation theory[31] of second order (MP2) and up to fourth orders including all single, double, triple, and quadruple excitations (MP4SDTQ) in single-point calculations. The geometries of all stationary point structures on the potential energy surfaces were fully optimized using analytical gradients at the SCF and MP2 level with both 6-31G* and 6-311G** basis sets. Electron correlation corrections were evaluated at the MP4 level based on the geometries optimized at the MP2/6-311G** level in the "frozen core" approximation. Total energies for open-shell systems were calculated with a projection method included in the Gaussian program and denoted by PMPn. The expectation values of $\langle S^2 \rangle$ were for UHF functions lower than 0.78, indicating minor spin contamination.

As in our preceding studies,[32] the total energies were improved using G2 (or its less sophisticated versions, G2MP2, G2MP3 and G1) formalism.[33] Vibrational frequencies obtained at the (U)HF/6-31G* level and scaled by 0.8929 were used in the calculation of the ideal-gas thermodynamic functions of reactants and transition states.

2.2. Molecular Structures. Optimized geometries and vibrational frequencies of intermediate structures obtained at the MP2/6-311G** level are given in Table 1 and shown in Figure 1. At all levels of theory, the search for the possible existence of intermediate complexes and transition states was made independently.

$CH_3OH + H$ Reaction System. Two transition states have been found, $CH_3O\cdots H\cdots H$ (**TS1**) and $H\cdots H\cdots CH_2OH$ (**TS2**) (Figure 1), depending on the H atom in the methanol which will be abstracted. The optimized structure of the transition state for the hydroxyl-side hydrogen abstraction (TS1) retains the C_s symmetry of methanol, and conserves the geometrical parameters of the OCH_3 part of the isolated CH_3OH. The H-attack on the OH group shows a nearly collinear structure in TS1, with the $O\cdots H\cdots H$ angle of 166°−173° depending on the method of calculation. The elongation of the $O\cdots H_o$ bond by almost 0.3 Å (MP2 level) corresponds to a relative increase of 31% in TS1 compared to the $O-H_o$ bond length in isolated CH_3OH molecule. Moreover, the forming $H\cdots H$ bond length in TS1 is 30% longer in comparison with the H−H bond in H_2 molecule. This is consistent with the fact that the reaction is nearly thermoneutral. As a result of the rotation of the methyl group of methanol, only one $H\cdots H\cdots CH_2OH$ (**TS2**) transition state structure was found for H-attack either on the antihydrogen of CH_3 (toward OH orientation) or on the synhydrogens. At all levels of theory, the H-attack on the methyl side is found almost collinear. The $C-H_1$ bond length in TS2 is longer by ca. 0.3 Å compared to that in methanol, which corresponds to a relative increase of 25%. The $H\cdots H_1$ bond length in TS2 is about 25% longer than that in the isolated H_2 molecule. A little shortening of the C−O bond length of 0.03 Å is also observed in the TS2 structure, but the $O-H_o$ bond length remains almost the same as in methanol. Except for the imaginary frequency, which

TABLE 1: Optimized Structures and Vibrational Frequencies of Stationary Points of the Potential Energy Surface Obtained at the MP2/6-311G Level[a]**

	TS1	TS2	TS3	TS4	TS5	TS6	MC6
C_1O_1	1.4031	1.3827	1.4011	1.3970	1.4181	1.4005	1.3584
O_1H_o	1.2554	0.9595	1.2479	0.9592	1.0733	0.9590	0.9682
C_1H_1	1.0955	1.3399	1.0965	1.2864	1.0933	1.1814	
C_1H_2	1.0955	1.0945	1.0974	1.0894	1.0951	1.0920	1.0816
C_1H_3	1.0961	1.0879	1.0974	1.0965	1.0928	1.0920	1.0869
H_oH	0.8450						
H_1H		0.9326					
CO_1			2.4677				
C_1C				2.6748			
OH_o					1.2348		1.8407
OH_1						1.3644	0.9595
OH					0.9656	0.9670	0.9592
CH_4			1.0883	1.0877			
CH_5			1.0884	1.0875			
CH_6			1.0882	1.0882			
$C_1O_1H_o$	106.3998	107.3530	105.8648	106.8231	107.5153	106.0863	106.5702
$O_1C_1H_1$	112.8418	110.6831	105.4599	110.0370	112.0351	110.4052	
$O_1C_1H_2$	112.8418	115.5884	112.8917	108.8586	111.9761	111.2935	113.8206
$O_1C_1H_3$	104.6083	109.8492	112.9746	114.5448	105.8531	111.2935	118.0065
O_1H_oH	166.6427						
CH_1H		178.4665					
C_1O_1C			101.6593				
OC_1C				107.8477			
O_1CH_4			108.3346				
O_1CH_5			102.7745				
O_1CH_6			106.5264				
C_1CH_4				107.3137			
C_1CH_5				102.0269			
C_1CH_6				105.2299			
O_1H_oO					146.6521		167.9034
H_oOH					100.3257		118.2587
OH_1C_1						155.0730	
HOH_1						92.8907	
H_1OH_o							112.5797
$H_oO_1C_1H_1$	62.7171	71.6533	178.2716	67.6905	−61.5420	67.9727	
$H_oO_1C_1H_2$	−62.7171	−45.0511	60.7648	−177.2176	61.5420	−49.6323	25.4202
$H_oO_1C_1H_3$	180.0000	−174.7780	−64.0885	−51.1778	180.0000	−174.4223	172.4379
$HH_oO_1C_1$	0.0000						
$HH_1C_1O_1$		−13.1104					
$H_1C_1O_1C$			178.7318				
$C_1O_1CH_4$			151.5627				
$C_1O_1CH_5$			32.1975				
$C_1O_1CH_6$			−86.6916				
$H_oO_1C_1C$				68.3317			
$O_1C_1CH_4$				167.6680			
$O_1C_1CH_5$				47.7546			
$O_1C_1CH_6$				−71.0926			
$OH_oO_1C_1$					70.5342		2.0367
HOH_oO_1					47.3044		−70.3824
$OH_1C_1O_1$						−1.5100	
HOH_1C_1						37.2184	
$H_1OH_oO_1$							50.8034
ν_1	226	299	26	45	131	126	103
ν_2	424	388	162	86	220	161	105
ν_3	660	572	185	260	253	274	152
ν_4	1022	1102	362	395	447	446	221
ν_5	1070	1122	579	508	863	752	272
ν_6	1195	1172	673	589	1069	942	328
ν_7	1200	1286	1089	690	1148	1079	718
ν_8	1468	1298	1165	1110	1198	1169	826
ν_9	1471	1411	1196	1149	1320	1324	1135
ν_{10}	1543	1520	1201	1171	1486	1361	1260
ν_{11}	2232	1608	1264	1220	1503	1421	1476
ν_{12}	3047	3093	1409	1398	1531	1509	1526
ν_{13}	3136	3227	1468	1430	1583	1612	1651
ν_{14}	3139	3909	1471	1441	3064	3107	3155
ν_{15}	2246 i	1827 i	1476	1475	3150	3197	3304
ν_{16}			1499	1484	3171	3844	3752
ν_{17}			1541	1519	3870	3916	3892
ν_{18}			3031	3072	2808 i	1599 i	4001
ν_{19}			3110	3108			
ν_{20}			3110	3203			
ν_{21}			3127	3256			
ν_{22}			3251	3262			
ν_{23}			3254	3911			
ν_{24}			2298 i	1958 i			

[a] Bond lengths in Å, valence and dihedral angles in degrees, vibrational frequencies in cm^{-1}.

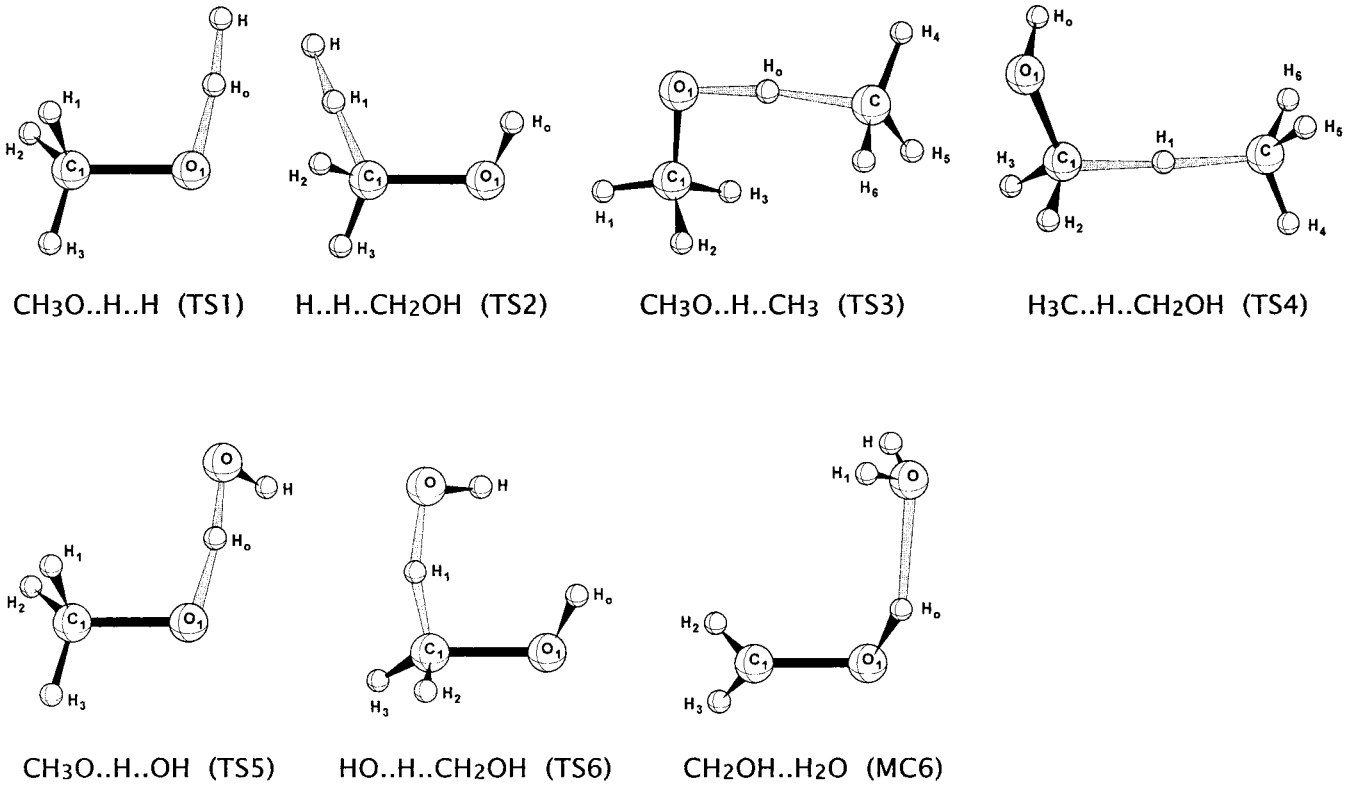

Figure 1. Configurations of the intermediate structures.

describes the move of the hydrogen of the methyl group between C and the H attacking atom, the other frequencies of TS2 are indeed similar to those of the isolated methanol.

CH_3OH + CH_3 Reaction System. The optimized structural parameters for the $CH_3O\cdots H\cdots CH_3$ (**TS3**) transition state only slightly depend either on the level of calculation or the basis set used. The structural parameters of TS3 are close to those obtained by Tachikawa et al.[16] using the MP2/6-31G calculation. The attack of the methyl radical carbon on the hydroxylic H-atom leads to an almost collinear arrangement of the $O-H_o\cdot\cdot\cdot C$ sequence in the TS3 structure. Except for MP2/6-311G** results, a C_s symmetry of methanol is found for the optimized structure of TS3. The symmetry plane C_1O_1C disappears in the MP2/6-311G** structure, and the attacking methyl group is distorted by about 30° from the ideal trans configuration. The breaking $O\cdots H_o$ bond length is elongated by 0.29 Å (29%) compared to its length in the isolated methanol molecule. A relative elongation of 25% of the $C-H_o$ bond compared to its value in methane is obtained. Values of the other structural parameters of TS3 are close for all the methods used. The optimized structure of $H_3C\cdots H\cdots CH_2OH$ (**TS4**) shows that the attack of the methyl radical on the hydrogen atom from the methyl side of methanol is nearly collinear. The bond lengths are close to those derived by Tachikawa et al.,[16] but the valence and dihedral angles cannot be compared because a C_s symmetry was imposed in their calculation. The bond distance for the forming $C\cdots H_1$ bond is the same for all methods used, i.e., 1.39 Å. It corresponds to an elongation of 30% compared to methane. There is no substantial difference in the values of the other structural parameters of TS3 obtained at different levels of theory. The normal modes having the imaginary frequency are the $O-H_o\cdots C$ asymmetric stretching for TS3 and the $C_1-H_1\cdot\cdot\cdot C$ asymmetric stretching for TS4 correspond to the reaction coordinates. The magnitude of the imaginary frequency is inversely correlated to the thickness of the potential barrier in the vicinity of the transition state along the reaction coordinate. A comparison of the imaginary frequencies of the two transition states indicates that considerably higher tunneling probability can be expected for the methoxy reaction channel. Values of the imaginary frequencies depend significantly on the level of theory used. The inclusion of electron correlation at the MP2 level decreases the imaginary frequency by about 30% and 25% compared to those obtained in SCF calculation for TS3 and TS4, respectively.

CH_3OH + OH Reaction System. The length of the breaking bond, O_1-H_o, the bond distance for the forming $O\cdots H_o$ bond, and the O_1-H_o-O angle are the revealing geometrical parameters of the $CH_3O\cdots H\cdots OH$ (**TS5**) transition state. The attack of the hydroxyl radical on the hydrogen of the hydroxyl group in methanol is not collinear. The O_1-H_o-O angle is of 140−145°, depending on the level of calculations. The SCF calculation leads to a C−H bond distance which is longer by 0.05 Å and an $O-H_o$ bond distance which is shorter by 0.05 Å than those obtained in MP2 calculations. On the other hand, the $O_1\cdot\cdot\cdot O$ distance in TS5 is very close at any level of theory. As obtained at MP2/6-311G** level, the bond length O_1-H_o = 1.073 Å and the $O-H_o$ distance equals 1.235 Å, corresponding to elongations of 12% and 30%, respectively, in comparison with the O−H bond lengths in isolated CH_3OH and H_2O molecules. This transition state is therefore reactant-like, which is consistent with the fact that the reaction is very exothermic. The optimized structure of $HO\cdots H\cdots CH_2OH$ (**TS6**) describes the attack of the hydroxyl radical on the methyl side of methanol. Similar to TS5, the MP2 calculation leads to an optimized TS6 structure where the O_1-H_1 breaking bond is shorter by 0.1 Å and the forming $O\cdots H_1$ bond is longer by 0.1 Å than those obtained in SCF calculation. The angle $O-H_1-C$ of 155° obtained in the MP2 calculation increases to ca. 170° at the SCF level. The imaginary frequency of TS6 is significantly lower than that of TS5.

A weakly bonded molecular complex $H_2O\cdots HOCH_2$ (**MC6**) has also been found in the exit channel leading to the

TABLE 2: Relative Energies, with Respect to Reactants Energy of Stationary Points of the Potential Energy Surface at 0 K for $CH_3OH + H$, CH_3, and OH Reaction Systems at Different Levels of Theory[a]

molecular system	PMP2[b]	MP4[c]	G2MP2	G2MP3	G1	G2	exptl[d]
$CH_2OH + H_2$	−5.3	−7.4	−8.1	−8.5	−7.6	−8.2	
	−4.8	***−6.8***	***−7.5***	***−7.9***	***−7.0***	***−7.6***	-7.9 ± 1.0
$H\cdots H\cdots CH_2OH$ (TS2)	10.2	10.1	9.0	8.8	9.6	9.0	
$CH_3O\cdots H\cdots H$ (TS1)	18.5	15.5	14.6	14.0	14.3	14.1	
$CH_3O + H_2$	5.7	0.0	1.2	0.2	0.8	0.6	
	6.1	***0.4***	***1.6***	***0.6***	***1.2***	***1.0***	1.2 ± 1.0
$CH_2OH + CH_4$	−8.2	−8.2	−7.8	−8.0	−7.7	−7.8	
	−8.4	***−8.4***	***−8.1***	***−8.3***	***−8.0***	***−8.1***	-8.6 ± 1.0
$H_3C\cdots H\cdots CH_2OH$ (TS4)	12.5	13.9	14.1	14.1	13.9	14.0	
$CH_3O\cdots H\cdots CH_3$ (TS3)	14.1	13.0	14.0	13.8	13.0	13.6	
$CH_3O + CH_4$	2.8	−0.8	1.6	0.7	0.6	1.0	
	2.5	***−1.2***	***1.1***	***0.2***	***0.1***	***0.5***	0.5 ± 1.0
$CH_2OH + H_2O$	−21.9	−18.3	−22.4	−21.6	−20.9	−21.8	
	−21.6	***−18.0***	***−22.1***	***−21.3***	***−20.6***	***−21.5***	-23.0 ± 1.0
$H_2O\cdots HOCH_2$ (MC6)	−28.9	−25.1	−26.9	−26.5	−26.0	−26.5	
$HO\cdots H\cdots CH_2OH$ (TS6)	3.2	4.4	1.0	1.3	1.0	0.9	
$CH_3O\cdots H\cdots OH$ (TS5)	3.8	5.1	3.6	3.7	3.2	3.5	
$CH_3O + H_2O$	−10.9	−10.9	−13.0	−12.9	−12.5	−13.0	
	−10.7	***−10.7***	***−12.9***	***−12.8***	***−12.4***	***−12.9***	-13.9 ± 1.0

[a] In kcal/mol; bold italic type (in product rows) shows the reaction enthalpy at 298 K. [b] PMP2/6-311G**//MP2/6−311G** energy with ZPE calculated using the unscaled MP2/6-311G** frequencies. [c] MP4SDTQ/6-311G**//MP2/6-311G** energy with ZPE calculated using the nonscaled MP2/6-311G** frequencies. [d] Calculated using the enthalpies of formation from refs 2 and 35.

hydroxymethyl radical. The geometrical parameters of MC6 are close to those derived for the isolated CH_2OH and H_2O species. The contact distance, $O\cdots H_o$ of 1.84−1.96 Å corresponds to a double elongation of the O−H bond in the water molecule. The vibrational levels of MC6, except the lowest ones, are also close to the corresponding frequencies of hydroxymethyl channel products. MC6 is a hydrogen bonded complex where the $O_1-H_o\cdots O$ atoms are almost collinear whatever the level of theory. Hydrogen bridged complexes between the hydroxymethyl channel products were also found in the reactions of methanol with F, Cl, and Br but with different structures.[32]

2.3. Energetics and Mechanism. Table 2 shows computational details of the relative energies with respect to reactant energies calculated at different levels of theory and with different basis sets. The mechanism of the H-abstraction from methanol by H and CH_3 is simple because no intermediate molecular complexes involving the reactants or products are formed. The branching products are then formed directly. The H-abstraction in the $CH_3OH + OH$ reaction system is a more complex process. The reaction channel which produces methoxy radicals (R5) is a simple metathesis reaction, but the formation of the hydroxymethyl radical (channel (R6)) may involve the formation of a hydrogen bonded complex. A comparison of the calculated energies of the stationary points at 0 K, as well as the reaction enthalpies at room temperature are given in Table 2.

$CH_3OH + H$ Reaction System. The calculated reaction enthalpies, for H-abstraction from methanol by hydrogen atoms, obtained at the MP4/6-311G** level and using the G2 methodology, are close to the experimental values (derived on the basis of the enthalpy of formation of reactants and products) for both reaction channels. Indeed, the simplified G2 procedures, G2MP2, G2MP3, and G1, yield energies very close to the "exact" G2 energy, which confirms that the use of the G2MP2 method is the most economic way for improvement of reaction energetics. The G2 method predicts the lowest energy barriers for both reaction channels, which are more than 1 kcal/mol lower than those obtained with the MP4/6-311G** approach. The calculations show that the reaction between H and CH_3OH occurs through sizable energy barriers giving rise to low rate constants for both CH_3O and CH_2OH reaction channels. It is in line with the results of kinetic measurements[3] and of a recent theoretical study of Lendvay et al. obtained by using G2 and BAC-MP4[36] (bond additivity correction of MP4 calculations) methods. The energy profile for the $CH_3OH + H$ reaction system obtained at the G2 level is shown in Figure 2. According to the relative difference in energy between TS5 and TS6, one can expect a dominance of the hydroxymethyl reaction channel (R2) over the methoxy formation (R1) at least in the low-temperature range.

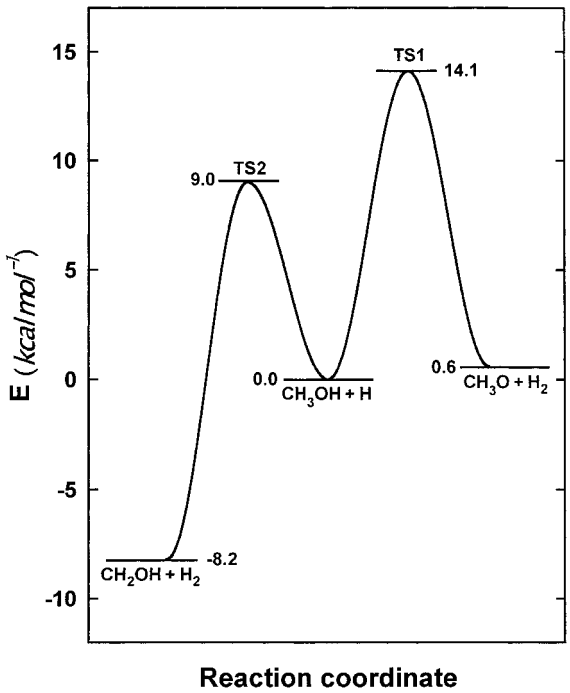

Figure 2. Schematic energy profile of the potential energy surface for the $CH_3OH + H$ reaction obtained at the G2 level.

$CH_3OH + CH_3$ Reaction System. All the methods which include the correlation energy lead to correct values of calculated reaction enthalpy for the hydroxymethyl reaction channel. The best heat of reaction for the methoxy channel was reached at G1 and G2 levels. Except for the MP2/6-311G** results, the calculations show that the lower energy barrier corresponds to the methoxy formation (R3). The best values of the energy

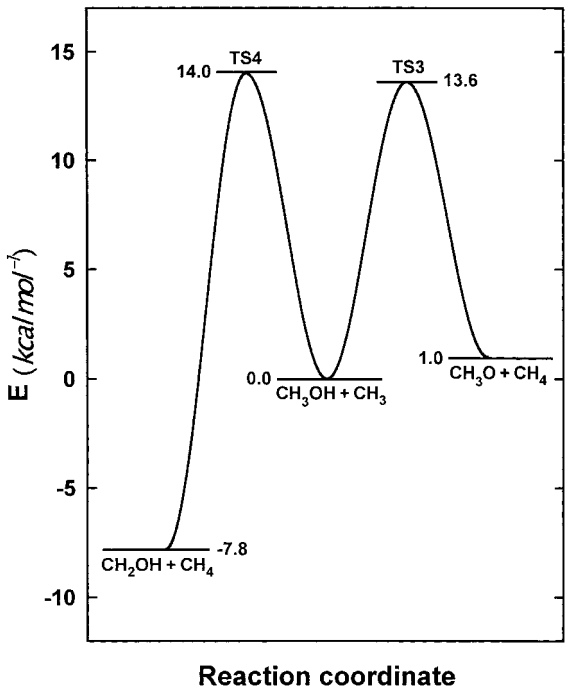

Figure 3. Schematic energy profile of the potential energy surface for the $CH_3OH + CH_3$ reaction obtained at the G2 level.

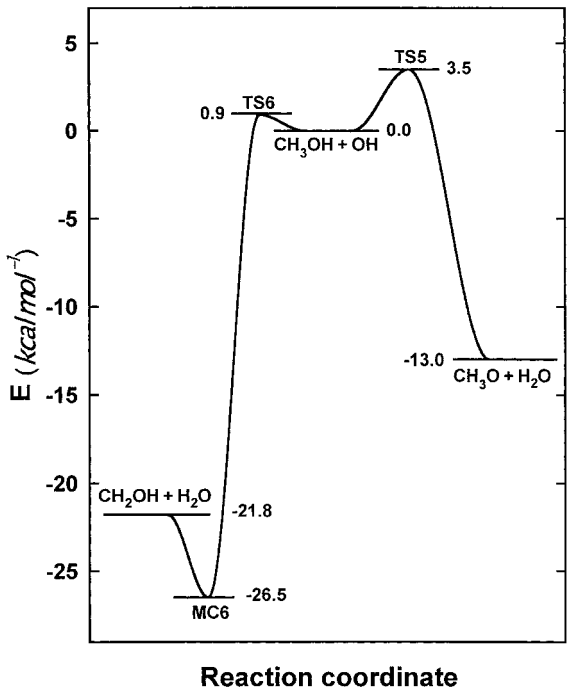

Figure 4. Schematic energy profile of the potential energy surface for the $CH_3OH + OH$ reaction obtained at the G2 level.

barriers, 13.6 kcal/mol for R3 reaction and 14.0 kcal/mol for R4 reaction, obtained by the most sophisticated G2 method, seem to be the most realistic values for further rate constant calculations. These values can be compared with energy barriers of 14.7 (R3) and 18.6 kcal/mol (R4) derived by Tachikawa et al.[16] at the MP4/6-31G**//MP2/6-31G level. However, the significant difference in the energy barriers is due to the fact that Tachikawa et al.[16] have assumed a C_s symmetry for the transition states. Our calculations show that the difference in the energies of the transition states, TS3 and TS4, is definitely smaller when symmetry restrictions are released in the saddle point searching procedure. The energy profile obtained at the G2 level is shown in Figure 3. The high energy barriers, which are only slightly different for the two reaction channels, imply lower overall rate constants compared to the $CH_3OH + H$ reaction system. Statistical considerations suggest a 3:1 dominance of the hydroxymethyl channel (R4).

$CH_3OH + OH$ Reaction System. As shown in Table 2, the use of the G2 methodology allows a significant improvement in the reaction energetics. This is especially evident for the methoxy reaction channel. The use of the G2 method leads to 1 kcal/mol difference between calculated reaction enthalpy and experiment for this reaction channel. Both reaction channels are strongly exothermic. The heights of the reaction barriers are relatively low, and they depend significantly on the method of calculation. At any level of theory the barrier for the reaction channel (R6), which leads to the formation of the hydroxymethyl radical, is lower than that for the methoxy channel (R5). The lowest energy barriers are those calculated in the G2 approach. Moreover, at this highest level of theory, the greatest difference in the energy barriers is observed for the two competing reaction channels. The heights of energy barriers at the G2 level are 3.5 and 0.9 kcal/mol for R5 and R6, respectively. In Figure 4 is shown the potential energy profile at 0 K obtained with the G2 methodology in the total energy calculation. On the basis of this potential energy profile, the mechanism of the reaction channel leading to the formation of hydroxymethyl radicals is expected to be rather complex. The transition state structure, identified by the calculations and designated by TS6, is a characteristic structure of a simple metathesis reaction. This suggests that the direct H atom abstraction from the methyl group occurs in the $CH_3OH + OH$ system. However, a second reaction path may also exist which leads to the $CH_2OH + H_2O$ products via a weakly bonded molecular complex, MC6. The formation of the complex is the rate-determining process in the two-step mechanism of (R6) in the $CH_3OH + OH$ reaction system. The molecular complex, MC6, is located on the energy scale (at G2 level) at 4.7 kcal/mol below the channel products. The back reaction of the complex formation (i.e., MC6 → reactants) can only be competitive with respect to the forward reaction (i.e., MC6 → products) at very high temperature. At low temperatures, the reverse process is negligible because the dominant part of MC6 undergoes decomposition to the final channel products. The small energy barriers calculated for both (R5) and (R6) reaction channels make probable the assumption that the $CH_3OH + OH$ reaction should proceed fast with a quite high overall rate constant, a few orders of magnitude higher than those for methanol reactions with hydrogen and methyl. The very low energy barrier for the hydroxymethyl channel suggests the dominance of this reaction channel.

2.4. Electronic Structures and Polar Effects. The heights of the energy barriers are clearly the major factors in determining the radical−methanol reactivity. To gain some insight into the reasons responsible for the differences in the energy barriers, and therefore in the rate constants, the change of the electronic distribution between reactants and the transition states has been carefully analyzed for the reactions studied. Table 3 contains the electronic net charge distribution on the selected atoms in the reactants and in the transition states obtained at the MP2/6-311G** level using Mulliken population analysis. It can provide some help in the description of changes of the electronic structure during the reaction.

The methanol molecule and the transition states of the reactions studied are polar structures. The polarity of the breaking C−H and O−H bonds is determined by the net charges on the C and O atoms (of the methanol part of the structure),

TABLE 3: Net Charge Distribution on the Selected Atoms in Reactants and Transition States

		net charge distribution on the atoms of						
molecule	atom	reactants	TS1	TS2	TS3	TS4	TS5	TS6
CH_3OH	C	0.003852	−0.022161	0.032338	−0.029413	0.012359	0.008370	−0.040451
	O	−0.471367	−0.310914	−0.430691	−0.334930	−0.452316	−0.491874	−0.468533
H	X[a]	0.000000	−0.096666	−0.077311				
CH_3	X[a]	−0.337146			−0.395017	−0.351610		
OH	X[a]	−0.250684					−0.310382	−0.325977
	δ(C)[b]			0.028486		0.008507		−0.044303
	δ(O)[b]		0.160453		0.136437		−0.020507	
	δ(X)[b]		−0.096666	−0.077311	−0.057871	−0.014464	−0.059698	−0.075293
	δ(C) + δ(X)[b]			−0.048825		−0.005957		−0.119596
	δ(O) + δ(X)[b]		0.063787		0.078566		−0.080205	
	V_o[c]		14.1	9.0	13.6	14.0	3.5	0.9

[a] X denotes the attacking atom, i.e., H, C of CH_3, and O of OH. [b] Structural parameters defined in section 3.4. [c] The energy barrier at 0 K calculated at G2 level in kcal/mol.

respectively. Let us denote by X the attacking atom or the atom of the attacking radical which forms a new bond with the abstracted hydrogen of methanol, i.e., X = H, C of CH_3, and O of OH for reaction of methanol with H, CH_3, and OH, respectively. The attack of H or CH_3 on the hydroxyl side of methanol causes a significant decrease of the electron density on oxygen at the respective transition state, i.e., the oxygen atom becomes less negative. This charge shift leads to a decrease of the charge on the abstracted H_o atom, whereas the attacking atom, X, becomes more negative in TS1 and TS3 structures than in isolated reactants, CH_3OH/H and CH_3OH/CH_3. The attack of an electrophilic OH radical is manifested for the TS5 structure by more negative charge on both oxygen atoms (of methanol and the attacking OH) with an increase of the positive charge on the abstracted H_o atom, of the methanol and on the hydrogen atom of the approaching radical OH.

The charge density on the attacking atom X in the transition states of the hydroxymethyl forming channels (TS2, TS4, and TS6) differs considerably from that derived for the isolated H, CH_3, and OH. It is interesting to note that the electronic density on the attacking atom, X, increases for all transition states of this channel, significantly in the case of reactions of methanol with H (TS2) and OH (TS6) and only slightly for the reaction with CH_3 (TS4). The shift of the electronic density is manifested by a change of the net charge distribution on atoms of methanol's methyl group of the transition state structures. The carbon atom of the breaking C−H bond becomes more positive in the H···H···CH_2OH (TS2) and H_3C···H···CH_2OH (TS4) structures compared to the isolated methanol and is negative in HO···H···CH_2OH (TS6).

To get a more detailed analysis about the relative importance of the charge shift caused by the approach of the atom/radical toward methanol, we have calculated the difference $\delta(A) = q_{TS}(A) - q_o(A)$, which describes the change of the electronic net charge on atom A at the transition state, $q_{TS}(A)$ compared to the isolated reactants, $q_o(A)$. In Table 3 are given these differences calculated for C and O atoms of methanol and the attacking atom, X. Values of $\delta(A)$ for those atoms seem to be a sensitive measure of the change in the electronic charge distribution related to the formation of O···H···X and C···H···X bonds at transition states and can be used to find a correlation with the energy barrier. A linear correlation can be drawn between $\delta(O) + \delta(X)$ or $\delta(C) + \delta(X)$ and the energy barrier for the methoxy and hydroxymethyl reaction channels. These correlations are shown in parts a and b of Figures 5. The energy barrier for the approach toward the hydroxyl side of the methanol is also well correlated with the change of the net charge on oxygen atom, $\delta(O)$. The credibility of those correlations obtained from a very limited number of the analyzed reactions (three points only) is supported by the fact that the correlation factors are close to unity. In general, the change in the net charge distribution expressed in terms of the structural indexes, $\delta(C)$, $\delta(O)$, and $\delta(X)$ determines the height of the reaction barrier. Derived structural indexes well explain the differences in relative reactivity of H, CH_3, and OH toward methanol.

In the cases of H and CH_3 reactions, a qualitative interpretation can be made between the comparative heights of TS1 versus TS2 and TS3 versus TS4 according to the hydrogen atom which will be abstracted from methanol. As can be seen from Table 1, the C−O bond distance is shorter in TS2 than in TS1, revealing the beginning of the formation of a double bond and a possible stabilization of TS2 more important than for TS1. Moreover, as shown in Table 3, the net charges $\delta(C)$ and $\delta(O)$ are both negative in TS1, whereas in TS2, $\delta(C)$ is slightly positive. These observations seem to argue in favor of a larger stabilization of TS2 with respect to TS1 and are in agreement with the fact that TS2 is lower in energy. In the case of TS3 and TS4, a similar reasoning can be made, but the differences are not so important and the interpretation is more difficult.

3. Rate Constant Calculations

The rate constant for the reaction channels (R1−R5) can be analyzed in terms of conventional transition state theory. The thermochemical formulation of transition state theory[37,38] leads to the rate constant, $k_{i,TST}$, given by

$$k_{i,TST} = \sigma \frac{k_B T}{h} \exp(\Delta S_i^{\neq}/R) \exp(-\Delta H_i^{\neq}/RT) \qquad (1)$$

where σ is the symmetry factor, k_B and h are the Boltzmann and Planck constants, respectively, $\Delta S_i^{\neq}$ is the activation entropy, and $\Delta H_i^{\neq}$ is the activation enthalpy for the corresponding reaction, i (i = R1−R5). The symmetry factor σ is related to the reaction path degeneracy and was taken to be equal to 3 and 1 for the hydroxymethyl and the methoxy reaction channels, respectively. Vibrational and rotational contributions to the thermodynamic functions in eq 1 were derived by the classical harmonic oscillator rigid rotor approximation (no free or internal rotation has been considered).[37] The molecular parameters used in the rate constant calculation were those obtained by the most sophisticated G2 method, i.e., the scaled (U)HF/6-31G* vibrational frequencies and the rotational constants obtained in the MP2/6-31G* geometry optimization.

A common practice in rate constant calculations for reactions with hydrogen transfer is to take into account a tunneling

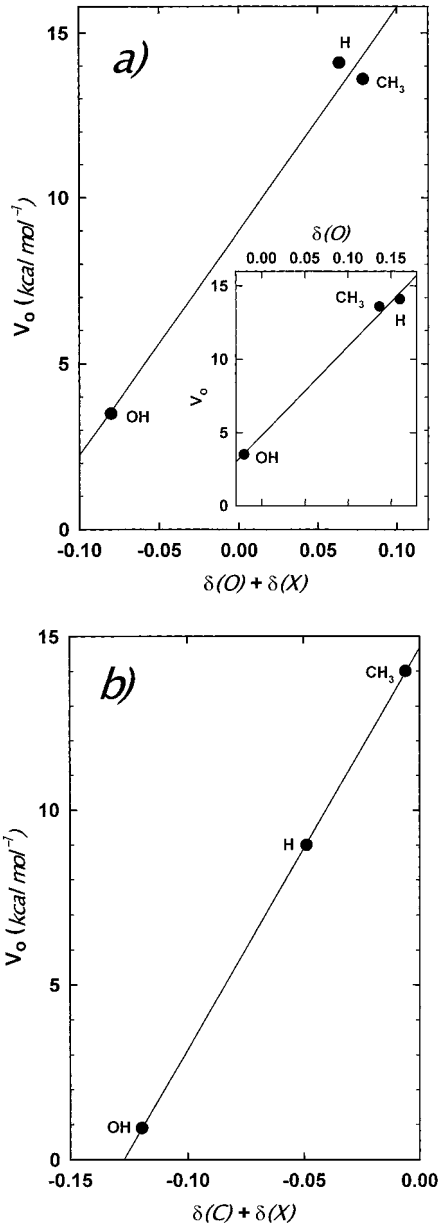

Figure 5. (a) Height of the energy barriers, V_o, versus the structural parameters, $\delta(O) + \delta(X)$ for the methoxy reaction channels (R1, R2, and R5). The linear regression equation is $y = 67.65x + 8.999$, and the correlation coefficient $R = 0.9921$. The insert shows the plot V_o vs $\delta(O)$; $y = 60.66x + 4.812$, $R = 0.9967$. (b) Plot of the energy barrier, V_o, versus the structural parameters $\delta(C) + \delta(X)$ for the hydroxymethyl reaction channels (R2, R4, and R6). Derived linear regression line: $y = 115.2x + 14.662$, and $R = 1.0000$.

effect,[38] which is usually represented by the tunneling correction factor, κ_i, as

$$k_i = \kappa_i k_{i,TST} \tag{2}$$

For reactions with high energy barriers, consideration of a tunneling effect may significantly improve the values of the calculated rate constants, especially at low temperatures. A reasonable correction of the rate constant may be obtained, even in a one-dimensional approximation, using the method described by Johnston et al.[38] with the Eckart type of potential. In this approach, the unsymmetrical potential is characterized by the forward and backward barrier heights and the imaginary frequency of the transition state.

A general equation for the rate constant calculation in the case of a bimolecular reaction proceeding through the formation of intermediate complexes was derived in a preceding paper (part 1).[32] According to this formalism, the rate constant for the formation of hydroxymethyl (channel R6) in the CH_3OH + OH reaction system can be written

$$k_{R6} = \frac{z}{hQ_AQ_B}\int_{V_{ts}}^{\infty} dE \sum_{J=0}^{J_m}\sum_{K=0}^{K_m} W_{ts}(E,J,K) \times \frac{W_{ac}(E,J,K)}{W_{ts}(E,J,K) + W_{ac}(E,J,K)} \exp(-E/RT) \tag{3}$$

where Q_A and Q_B are the partition functions of CH_3OH and OH, respectively, with the center of mass partition function factored out of the product Q_AQ_B and included in z together with the partition functions of those inactive degrees of freedom which are not considered by the sums of the states under the integral. $W_{ts}(E,J,K)$ and $W_{ac}(E,J,K)$ denote the sum of the states at energy less than or equal to E and angular momentum quantum numbers J and K, for the transition state TS6 (ts) and an "activated complex" (ac) for unimolecular dissociation of MC6 to channel products, respectively. V_{ts} is the threshold energy for the first elementary step at angular momentum $J = 0$. If V_i ($i = as, ts$) denotes the potential energy of the transition state/activated complex and $U_i(J,K)$ is its rotational energy corresponding to angular momentum quantum numbers J and K, then the upper limit J_m at given E is given by the following conditions:

$$J_m(E) = \min_i\{J_i\} \tag{4a}$$

where J_i is the highest integer number satisfying the inequality

$$V_i + U_i(J_i,0) \le E \tag{4b}$$

At fixed E and J, the upper limit of K, K_m, is determined by

$$K_m(E,J) = \min_i\{K_i\} \tag{5a}$$

with K_i given by the conditions:

$$V_i + U_i(J,K_i) \le E \quad \text{and} \quad K_i \le J \tag{5b}$$

The sums of the states $W(E,J,K)$ were calculated in a classical harmonic oscillator and rigid rotor approximation. Rotational energy at given angular momentum (J,K) was derived for an assumed prolate symmetry top system. The microcanonical version of the statistical adiabatic channel model (SACM) developed by Troe[39] was used to derive the structural parameters of the activated complex, i.e., the centrifugal energy barriers, and the quanta of the "disappearing" and "conserved" oscillators. The sum of the vibrational states necessary for the calculation of $W(E,J,K)$ was evaluated by the inverse Laplace transformation of respective partition functions using the steepest descent method.[40] All the internal parameters of the SACM method used were determined by the molecular properties derived in ab initio calculation without fitting or adjustable parameters. The computational details related to calculation of rate constant and the method used for the description of unimolecular processes are discussed in detail in the part 1[32] of this series of papers.

3.1. CH_3OH + H Reaction System. The energy barriers for both reaction channels of CH_3OH + H are high, which implies either small values of rate constants or strong dependence on

TABLE 4: Calculated Rate Constants for Formation of Methoxy, k_{R1} and Hydroxymethyl, k_{R2} Radicals for $CH_3OH + H$ Reaction System and for the Inverse Reactions, k_{-R1} and k_{-R2}

T (K)	$k_{R1,TST}$ (cm^3 $molec^{-1}$ s^{-1})	k_{R1}	k_{R1} (cm^3 $molec^{-1}$ s^{-1})	K_1[a]	k_{-R1} (cm^3 $molec^{-1}$ s^{-1})	$k_{R2,TST}$ (cm^3 $molec^{-1}$ s^{-1})	k_{R2}	k_{R2} (cm^3 $molec^{-1}$ s^{-1})	K_2[b]	k_{-R2} (cm^3 $molec^{-1}$ s^{-1})
300	9.64×10^{-22}		(1.6×10^{-19})[c]		(1.9×10^{-19})[d]	1.40×10^{-17}	46.79	6.53×10^{-16}	2.76×10^{6}	2.36×10^{-22}
400	3.80×10^{-19}	27.18	1.03×10^{-17}	1.57	6.58×10^{-18}	6.57×10^{-16}	7.51	4.94×10^{-15}	1.20×10^{5}	4.12×10^{-20}
500	1.46×10^{-17}	7.29	1.07×10^{-16}	2.07	5.14×10^{-17}	7.15×10^{-15}	3.49	2.50×10^{-14}	1.91×10^{4}	1.31×10^{-18}
600	1.75×10^{-16}	3.82	6.70×10^{-16}	2.50	2.68×10^{-16}	3.73×10^{-14}	2.37	8.82×10^{-14}	5.73×10^{3}	1.54×10^{-17}
700	1.08×10^{-15}	2.65	2.86×10^{-15}	2.85	1.00×10^{-15}	1.27×10^{-13}	1.88	2.39×10^{-13}	2.45×10^{3}	9.78×10^{-17}
800	4.37×10^{-15}	2.10	9.19×10^{-15}	3.14	2.93×10^{-15}	3.31×10^{-13}	1.63	5.39×10^{-13}	1.30×10^{3}	4.16×10^{-16}
900	1.33×10^{-14}	1.81	2.41×10^{-14}	3.35	7.20×10^{-15}	7.16×10^{-13}	1.48	1.06×10^{-12}	7.88×10^{2}	1.34×10^{-15}
1000	3.32×10^{-14}	1.62	5.36×10^{-14}	3.52	1.52×10^{-14}	1.36×10^{-12}	1.38	1.88×10^{-12}	5.27×10^{2}	3.57×10^{-15}
1500	6.19×10^{-13}	1.27	7.86×10^{-13}	3.82	2.06×10^{-13}	1.11×10^{-11}	1.15	1.28×10^{-11}	1.49×10^{2}	8.64×10^{-14}
2000	3.16×10^{-12}	1.17	3.70×10^{-12}	3.71	9.96×10^{-13}	3.73×10^{-11}	1.10	4.12×10^{-11}	7.31×10^{1}	5.64×10^{-13}

[a] The equilibrium constant for $CH_3OH + H \leftrightarrow CH_3O + H_2$. [b] The equilibrium constant for $CH_3OH + H \leftrightarrow CH_2OH + H_2$. [c] Derived from eq 6. [d] Derived from eq 8.

TABLE 5: Values of Calculated and Experimental Overall Rate Constants, $k_{ov,calc}$ and $k_{ov,exp}$, and Theoretical Branching Ratio of the Hydroxymethyl Reaction Channel, $\Gamma(CH_2OH)$ for $CH_3OH + H$ Reaction[a]

T (K)	$k_{ov,calc}$ (cm^3 $molec^{-1}$ s^{-1})	$k_{ov,exp}$[b] (cm^3 $molec^{-1}$ s^{-1})	$\Gamma(CH_2OH)$
300	6.5×10^{-16}	1.7×10^{-15} $(1.2-3.0) \times 10^{-15}$	1.00
400	5.0×10^{-15}	2.4×10^{-14} $(1.2-2.8) \times 10^{-14}$	1.00
500	2.5×10^{-14}	1.3×10^{-13} 1.1×10^{-13}	1.00
600	8.9×10^{-14}	4.3×10^{-13} $(2.6-2.7) \times 10^{-13}$	0.99
700	2.4×10^{-13}	1.1×10^{-12} 5.0×10^{-13}	0.99
800	5.5×10^{-13}	2.2×10^{-12}	0.98
900	1.1×10^{-12}	4.0×10^{-12}	0.98
1000	1.9×10^{-12}	6.5×10^{-12} 1.5×10^{-12}	0.97
1500	1.4×10^{-11}	3.5×10^{-11} $(0.9-2.3) \times 10^{-11}$	0.94
2000	4.5×10^{-11}	9.5×10^{-11} $(1.4-2.9) \times 10^{-11}$	0.92

[a] $k_{ov} = k_{R1} + k_{R2}$; $\Gamma(CH_2OH) = k_{R2}/k_{ov}$. [b] Derived from Tsang[3] equation: $(3.52 \times 10^{-17})T^{2.11} \exp(-2450/T)$ (left column), and the range of experimental results from refs 5−8 and 10 (right column).

temperature. Results of the rate constant calculation for the $CH_3OH + H$ reaction system are given in Table 4. The rate constants were calculated, using conventional transition state theory, on the basis of eq 1. Molecular parameters of reactants and transition states used in the calculation were those derived at the G2 level, i.e., G2 total energies, scaled vibrational frequencies obtained in (U)HF/6-31G* calculation, and rotational constants corresponding to the MP2/6-31G* optimized geometries. The tunneling correction factor depends sensitively on the imaginary frequency used in the calculation. Since very high imaginary frequencies were obtained in the SCF calculations, we decided to evaluate the tunneling factors with the more realistic imaginary frequencies which were obtained at a higher level of theory, i.e., the unscaled MP2/6-311G** imaginary frequencies.

The results of calculations show that the reaction channel which leads to the formation of methoxy radicals (R1) is practically inactive in comparison with (R2) at temperatures below 1000 K. Both rate constants, k_{R1} and k_{R2} are small. The rate constant for the hydroxymethyl channel, $k_{R2} = 6.5 \times 10^{-16}$ cm^3 $molecule^{-1}$ s^{-1} is about 5 orders of magnitude lower than that of the analogous reaction channel for the slightly less exothermic reaction of methanol with chlorine.[32] Due to the high energy barriers, the calculated tunneling correction factors are very high at low temperatures. Therefore, we did not use the artifactly high tunneling correction factor for k_{R1} at 300 K. Available experimental rate constants were obtained in two different ranges of temperature: direct measurements[5−8] at 298−630 K and high-temperature data (above 1000 K) from shock tube experiments.[10] However, those two sets of measurements are difficult to compare. In general, an extrapolation of the high-temperature data leads to overestimation of the low-temperature rate constants, which suggests too low values of activation energy derived at high temperatures. The experimental results given in Table 5 are based on the kinetic data evaluation made by Tsang.[3] The Tsang equation[3] can be considered as the best compromise between the low- and high-temperature measurements and allows a gap of experimental data in the intermediate temperature range to be filled. However, Tsang's values seem to overestimate the rate constant over 1000 K. The temperature dependence of the calculated rate constants, k_{R1} and k_{R2} can be expressed, in terms of three-parameters fits of the form $A(T/300)^n \exp(-E/T)$, as follows:

$$k_{R1} = (3.0 \times 10^{-14})\,(T/300)^{3.4} \times \exp(-3640/T)\ \text{cm}^3\ \text{molecule}^{-1}\ \text{s}^{-1} \quad (6)$$

$$k_{R2} = (1.9 \times 10^{-13})\,(T/300)^{3.2} \times \exp(-1755/T)\ \text{cm}^3\ \text{molecule}^{-1}\ \text{s}^{-1} \quad (7)$$

The above equations allow reproduction of the values of the theoretical rate constants given in Table 4 with a precision sufficient for kinetic modeling. The relative errors do not exceed 15% for k_{R1} and 20% for k_{R2}. The fitting parameters are tightly correlated so that an Arrhenius activation energy cannot be derived. In such a type of fit, when the functional parameters A, n, and E are strongly coupled, even a little change of the input k values may lead to identical quality fits but with considerably different values of fitting parameters. This is especially important for an analysis of the usually scattered experimental rate constants. Therefore, even with very accurate experimental measurements, such three-parameter fits should be viewed only as shorthand representations of the kinetic data. Due to the high tunneling correction factor, the value of k_{R1} at 300 K was not calculated from eq 2. Extrapolation on the basis of eq 6 leads to a value of $k_{R1} = 1.6 \times 10^{-19}$ cm^3 $molecule^{-1}$ s^{-1} at 300 K. This is more than 3 orders of magnitude lower than that derived for the hydroxymethyl channel at the same temperature. A comparison of the calculated and experimental values of the overall rate constant, $k_{ov} = k_{R1} + k_{R2}$ (which is indeed equal to k_{R2} since k_{R1} is small) is shown in Figure 6. The relatively large value of n reflects a non-Arrhenius behavior of the theoretically derived rate constants. It is a result of the strong negative dependence on temperature of the derived tunneling factor. The calculated overall rate constant, k_{ov}, is in satisfactory agreement with that recommended by Tsang over the temperature range studied. However, the values calculated in this study are systematically lower than those derived from

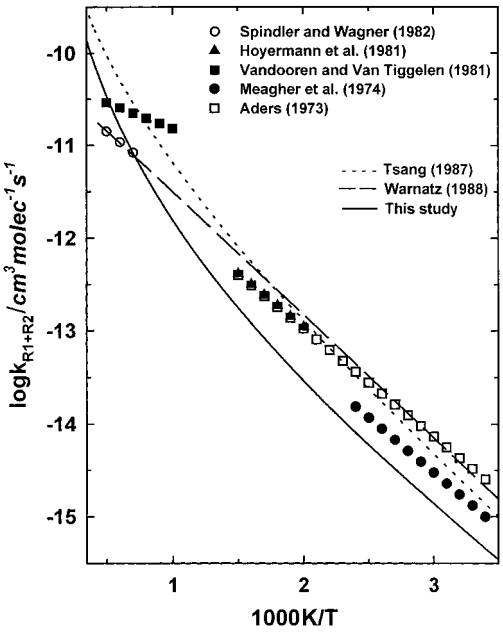

Figure 6. Arrhenius plot for the $CH_3OH + H$ reaction comparing kinetic measurements (symbols) with data evaluations (lines) in the functional form $AT^n\exp(-E/T)$ of Spindler and Wagner[10] (1600−2100 K, R1 + R2: $A = 5.3 \times 10^{-11}$, $n = 0$, $E = 2670$); Hoyermann et al.[5] (500−680 K, R1 + R2: 2.2×10^{-11}, 0, 2650); Vandooren and Van Tiggelen[7] (1000−2000 K, R1 + R2: 1000−2000 K, 5.6×10^{-11}, 0, 1309); Maegher et al.[6] (300−404 K, R1 + R2: 1.1×10^{-11}, 0, 2739); Aders[8] (298−650 K, R1 + R2: 2.2×10^{-11}, 0, 2669); Tsang[3] (300−2000 K, R1 + R2: 3.52×10^{-17}, 2.11, 2450); Warnatz[9] (300−2000 K, R1 + R2: 6.6×10^{-11}, 0, 3067); this study eqs 6 and 7.

the Tsang equation. The divergence is a factor of 3 at 300 K and becomes slightly worse in the intermediate temperature range, while it becomes better at high temperatures. In the high-temperature range, our calculated k_{ov} agrees within a factor of 2 with Tsang's recommendation. However, it is worth noting that values of k_{ov} obtained in this study are in better agreement with the high-temperature measurements[7,10] than those estimated from the Tsang equation. At 2000 K, the calculated k_{ov} of 4.5×10^{-11} cm^3 molecule^{-1} s^{-1} is 2 times lower than Tsang's recommendation of 9.5×10^{-11} cm^3 molecule^{-1} s^{-1}, which significantly overestimates the experimental results of 1.4×10^{-11} cm^3 molecule^{-1} s^{-1} of Spindler and Wagner[10] and 2.9×10^{-11} cm^3 molecule^{-1} s^{-1} of Vandooren and Van Tiggelen.[7] Lower values of the rate constant, k_{ov}, of 3.1×10^{-12} cm^3 molecule^{-1} s^{-1} and 1.4×10^{-11} cm^3 molecule^{-1} s^{-1} at 1000 and 2000 K, respectively, are also recommended by Warnatz[9] in his evaluation of kinetic data. On the other hand, in the intermediate temperature range, our calculated rate constants, k_{ov}, of 8.9×10^{-14} cm^3 molecule^{-1} s^{-1} and 2.4×10^{-13} cm^3 molecule^{-1} s^{-1} are about 3 and 2 times lower than the results of measurements at 600 and 700 K, respectively. Tsang's equation also yields in this temperature range overestimated values of the rate constant (of 60% at 600 K and 120% at 700 K), but well reproduces experimental results in the range 300−500 K. Therefore, our calculated rate constants allow a quite satisfactory description of $CH_3OH + H$ kinetics, especially in the high-temperature range. Calculated branching ratios indicate dominance of the hydroxymethyl channel at any temperature studied, and the formation of methoxy radicals is negligible at temperatures below 1000 K. This is in line with the recent theoretical results of Lendvay et al.[13] which show that the formation of hydroxymethyl radicals is the dominant route and 96%, 93% and 90% of methanol reacting with H atoms is converted into CH_2OH at 1000, 1500, and 2000 K, respectively. The values of the hydroxymethyl branching fraction calculated in this study of 97%, 94%, and 92% at the same temperatures agree very well with those derived by Lendvay et al.[13]

There are no experimental data available for reverse reactions related to hydrogen atom abstraction from hydrogen molecule by methoxy and hydroxymethyl radicals, $CH_3O + H_2 \rightarrow CH_3OH + H$ (−R1) and $CH_2OH + H_2 \rightarrow CH_3OH + H$ (−R2). Values of k_{-R1} and k_{-R2} given in Table 4 were derived on the basis of theoretically calculated equilibrium constants and can be expressed as

$$k_{-R1} = (1.7 \times 10^{-15})(T/300)^{4.0} \times \exp(-2470/T)\ \text{cm}^3\ \text{molecule}^{-1}\ \text{s}^{-1} \quad (8)$$

$$k_{-R2} = (8.8 \times 10^{-15})(T/300)^{3.5} \times \exp(-5270/T)\ \text{cm}^3\ \text{molecule}^{-1}\ \text{s}^{-1} \quad (9)$$

Both reactions proceed slowly with rate constants of 1.9×10^{-19} cm^3 molecule^{-1} s^{-1} and 2.4×10^{-22} cm^3 molecule^{-1} s^{-1} at 300 K for k_{-R1} and k_{-R2}, respectively. The almost zero reaction enthalpy for reactions (R1) and (−R1) leads to a value of the equilibrium constant, K_1, close to unity, which implies similar values of the rate constants, k_{R1} and k_{-R1}. The rate constant for the reverse reaction, k_{-R1}, is however more than 3 orders of magnitude lower than k_{-R2} and is only of minor importance in the $CH_3OH + H$ reaction system.

3.2. $CH_3OH + CH_3$ Reaction System. The energy profile for the $CH_3OH + CH_3$ reaction system shows high energy barriers for both reaction channels, leading to small values of the rate constants. As previously, the molecular parameters of methanol, methyl, and the two transition states, TS3 and TS4, obtained at the G2 level (with nonscaled imaginary MP2/6-311G** frequencies in the tunneling factor calculation), were used in the rate constant calculation. Results of the calculation are given in Table 6. As a result of the high barrier heights, the calculated rate constants both for methoxy, k_{R3}, and for hydroxymethyl, k_{R4}, reaction channels strongly depend on temperature. The tunneling factors at low temperatures (below 400 K) are very high, and they were not used in the calculations of the rate constants. Calculated values of k_{R4} are in very good agreement with those recommended by Tsang[3] and former evaluations of experimental kinetic data by Kerr and Personage[14] for the temperature range of 350−550 K. There are no experimental data available in the intermediate temperature range of 600−1500 K so that the results of our calculations can be useful in modeling studies. The temperature dependence of k_{R4} can be expressed in the form

$$k_{R4} = (1.4 \times 10^{-15})(T/300)^{4.9} \times \exp(-3380/T)\ \text{cm}^3\ \text{molecule}^{-1}\ \text{s}^{-1} \quad (10)$$

A relatively large value of the parameter n is related to the strong negative temperature dependence of the tunneling factor, as observed for the $CH_3OH + H$ reaction system.

Calculated rate constants for the methoxy reaction channel (R3) are systematically greater than those recommended by Tsang[3] and Kerr and Personage.[14] However, the discrepancy with Tsang's values does not exceed a factor of 2 in the experimentally most investigated temperature range of 350−550 K. If one takes into account that Tsang's recommended values for temperatures below 600 K are given with an uncertainty factor of 1.4, the agreement can be considered quite good. The temperature dependence obtained in this study for

TABLE 6: Calculated Rate Constants for Formation of Methoxy, k_{R3} and Hydroxymethyl, k_{R4} Radicals for $CH_3OH + CH_3$ Reaction System and for the Inverse Reactions, k_{-R3} and k_{-R4}

T (K)	$k_{R3,TST}$ (cm^3 $molec^{-1}$ s^{-1})	k_{R3}	k_{R3} (cm^3 $molec^{-1}$ s^{-1})	K_3[a]	k_{-R3} (cm^3 $molec^{-1}$ s^{-1})	$k_{R4,TST}$ (cm^3 $molec^{-1}$ s^{-1})	k_{R4}	k_{R4} (cm^3 $molec^{-1}$ s^{-1})	K_4[b]	k_{-R4} (cm^3 $molec^{-1}$ s^{-1})
300	9.07×10^{-23}		(1.7×10^{-20})[c]		(1.7×10^{-19})[d]	2.13×10^{-22}		(1.8×10^{-20})[e]		(7.9×10^{-26})[f]
350	2.44×10^{-21}		(1.4×10^{-19})[c]		(1.4×10^{-18})[d]	6.46×10^{-21}		(1.9×10^{-19})[e]		(6.0×10^{-24})[f]
400	2.98×10^{-20}	29.03	8.66×10^{-19}	9.67×10^{-2}	8.95×10^{-18}	8.68×10^{-20}	14.07	1.22×10^{-18}	7.38×10^{3}	1.65×10^{-22}
450	2.15×10^{-19}	13.24	2.84×10^{-18}	9.94×10^{-2}	2.86×10^{-17}	6.77×10^{-19}	7.26	4.91×10^{-18}	2.34×10^{3}	2.10×10^{-21}
500	1.07×10^{-18}	7.75	8.27×10^{-18}	1.00×10^{-1}	8.23×10^{-17}	3.61×10^{-18}	4.70	1.70×10^{-17}	9.25×10^{2}	1.83×10^{-20}
550	4.06×10^{-18}	5.30	2.15×10^{-17}	1.00×10^{-1}	2.14×10^{-16}	1.46×10^{-17}	3.49	5.08×10^{-17}	4.32×10^{2}	1.18×10^{-19}
600	1.26×10^{-17}	4.01	5.05×10^{-17}	9.96×10^{-2}	5.07×10^{-16}	4.76×10^{-17}	2.81	1.34×10^{-16}	2.28×10^{2}	5.85×10^{-19}
700	7.84×10^{-17}	2.76	2.16×10^{-16}	9.72×10^{-2}	2.22×10^{-15}	3.24×10^{-16}	2.10	6.79×10^{-16}	8.34×10^{1}	8.14×10^{-18}
800	3.27×10^{-16}	2.18	7.11×10^{-16}	9.44×10^{-2}	7.53×10^{-15}	1.45×10^{-15}	1.77	2.56×10^{-15}	3.90×10^{1}	6.56×10^{-17}
900	1.04×10^{-15}	1.85	1.92×10^{-15}	9.17×10^{-2}	2.09×10^{-14}	4.85×10^{-15}	1.56	7.58×10^{-15}	2.15×10^{1}	3.52×10^{-16}
1000	2.71×10^{-15}	1.66	4.49×10^{-15}	8.93×10^{-2}	5.03×10^{-14}	1.33×10^{-14}	1.45	1.92×10^{-14}	1.34×10^{1}	1.43×10^{-15}
1500	6.55×10^{-14}	1.27	8.30×10^{-14}	8.14×10^{-2}	1.02×10^{-12}	3.68×10^{-13}	1.20	4.42×10^{-13}	3.16	1.40×10^{-13}
2000	4.30×10^{-13}	1.16	4.98×10^{-13}	7.77×10^{-2}	6.41×10^{-12}	2.58×10^{-12}	1.13	2.91×10^{-12}	1.53	1.90×10^{-12}

[a] The equilibrium constant for $CH_3OH + CH_3 \leftrightarrow CH_3O + CH_4$. [b] The equilibrium constant for $CH_3OH + CH_3 \leftrightarrow CH_2OH + CH_4$. [c] Derived from eq 11. [d] Derived from eq 12. [e] Derived from eq 10. [f] Derived from eq 13.

k_{R3} is expressed by

$$k_{R3} = (2.7 \times 10^{-16})(T/300)^{4.7} \times \exp(-2910/T)\ \mathrm{cm^3\ molecule^{-1}\ s^{-1}} \quad (11)$$

Values of the calculated branching ratios change significantly with temperature. The slightly lower energy barrier for the methoxy reaction channel of 0.4 kcal/mol (at G2 level) enfeebles the statistically favored H-abstraction from the methyl group at low temperature. It leads to almost the same methoxy and hydroxymethyl fractions at room temperature. However, the fact that there are three possibilities of abstracting a hydrogen from the methyl group and only one from the hydroxyl group of the methanol leads to the dominance of the hydroxymethyl reaction channel when the temperature raises. Calculated branching ratios agree fairly well with the "experimental" values of Tsang[3] and Kerr and Personage[14] for temperatures higher than 500 K. Our calculated branching ratio of hydroxymethyl formation of 0.7 at 550 K is in excellent agreement with 0.71 and 0.77 derived on the basis of Kerr and Personage's and Tsang's equations, respectively. The overall rate constant, $k_{ov} = k_{R3} + k_{R4}$, is also very close to that recommended by Tsang for temperatures below 600 K. However, as it is shown in Figure 7 and Table 7, our k_{ov} shows a stronger increase with temperature. At 2000 K, k_{ov} calculated in this study is 1 order of magnitude higher than that predicted by Tsang but matches well the results of the high-temperature measurements of Spindler and Wagner.[10] The quantitative agreement which was reached between theoretical k_{ov} values and results of low- and high-temperature experiments proves the high quality of the rate constants k_{R3} and k_{R4} obtained in this study. Equations 10 and 11 describe successfully the kinetics of H-abstraction for the $CH_3OH + CH_3$ reaction system.

It is interesting to compare the results obtained for $CH_3OH + CH_3$ and for the analogous $CH_3OH + H$ reaction. Both reaction systems are characterized by similar reaction enthalpies for the corresponding reaction channels. However, the overall rate constant for the $CH_3OH + CH_3$ reaction is a few orders of magnitude lower than that for the reaction of methanol with hydrogen atoms. The calculated branching ratio for H-abstraction by methyl radicals depends sensitively on temperature. The increase of temperature leads to the dominance of the hydroxymethyl reaction channel. However, the methoxy radicals are formed with an efficiency not less than 15% at the highest temperature of this study (2000 K). Therefore, both methoxy and hydroxymethyl radicals should be observed experimentally as final products in the reaction of methanol with methyl radicals. The attack of methyl radicals on methanol is less selective compared to the $CH_3OH + H$ reaction which yields practically only hydroxymethyl channel products.

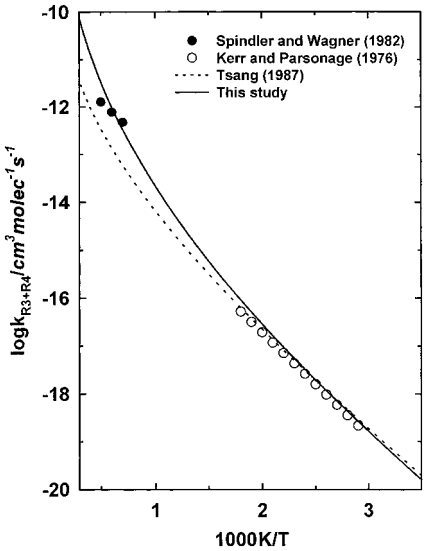

Figure 7. Arrhenius plot for the $CH_3OH + CH_3$ reaction comparing kinetic measurements (symbols) with data evaluations (lines) in the functional form $AT^n \exp(-E/T)$ of Spindler and Wagner[10] (1600−2100 K, R3 + R4: $A = 1.5 \times 10^{-11}$, $n = 0$, $E = 4940$); Kerr and Personage[14] (350−550 K, R3: 1.0×10^{-13}, 0, 4884; R4: 3.24×10^{-13}, 0, 5035); Tsang[3] (300−2000 K, R3: 2.4×10^{-23}, 3.1, 3490; R4: 5.3×10^{-23}, 3.17, 3609); this study eqs 10 and 11.

The inverse reactions of H-abstraction from methane by methoxy, $CH_3O + CH_4 \rightarrow CH_3OH + CH_3$ (−R3), and hydroxymethyl, $CH_2OH + CH_4 \rightarrow CH_3OH + CH_3$ (−R4), have not been investigated experimentally. The calculated k_{-R3} and k_{-R4} values are listed in Table 6. In the temperature range of 300−2000 K, these rate constants can be written in the following form:

$$k_{-R3} = (2.5 \times 10^{-15})(T/300)^{5.0} \times \exp(-2810/T)\ \mathrm{cm^3\ molecule^{-1}\ s^{-1}} \quad (12)$$

$$k_{-R4} = (5.2 \times 10^{-15})(T/300)^{5.0} \times \exp(-7475/T)\mathrm{cm^3\ molecule^{-1}\ s^{-1}} \quad (13)$$

Similar to the direct reactions, the reverse ones, (−R3) and (−R4), are slow processes. At 300 K, the rate of those processes

TABLE 7: Values of Calculated and Experimental Overall Rate Constants, $k_{ov,calc}$ and $k_{ov,exp}$, and Theoretical Branching Ratio of the Hydroxymethyl Reaction Channel, Γ(CH_2OH), for $CH_3OH + CH_3$ Reaction[a]

	$k_{ov,calc}$	$k_{ov,exp}$[b]		Γ(CH_2OH)	
T (K)	(cm^3 $molec^{-1}$ s^{-1})	(cm^3 $molec^{-1}$ s^{-1})		calcd	exptl[3]
300	3.4×10^{-20}	4.2×10^{-20}		0.52	0.76
350	3.3×10^{-19}	3.6×10^{-19}		0.58	0.76
400	2.1×10^{-18}	1.9×10^{-18}		0.59	0.76
450	7.8×10^{-18}	7.3×10^{-18}		0.63	0.76
500	2.5×10^{-17}	2.2×10^{-17}		0.67	0.77
550	7.2×10^{-17}	5.7×10^{-17}		0.70	0.77
600	1.8×10^{-16}	1.3×10^{-16}		0.73	0.77
700	9.0×10^{-16}	4.8×10^{-16}		0.76	0.77
800	3.3×10^{-15}	1.4×10^{-15}		0.78	0.77
900	9.5×10^{-15}	3.2×10^{-15}		0.80	0.78
1000	2.4×10^{-14}	6.6×10^{-15}		0.81	0.78
1500	5.3×10^{-13}	7.6×10^{-14}	5.6×10^{-13}	0.84	0.78
2000	3.4×10^{-12}	3.4×10^{-13}	1.3×10^{-12}	0.85	0.79

[a] $k_{ov} = k_{R3} + k_{R4}$; $\Gamma(CH_2OH) = k_{R4}/k_{ov}$. [b] From Tsang equations[3]: $(2.4 \times 10^{-23})T^{3.1} \exp(-3490/T) + (5.3 \times 10^{-23})T^{3.2} \exp(-3609/T)$ (left column) and from measurements of Spindler and Wagner[10] (right column).

is described by the rate constants of 1.6×10^{-19} cm^3 $molecule^{-1}$ s^{-1} and 6.5×10^{-26} cm^3 $molecule^{-1}$ s^{-1} for the −R3 and −R4 reactions, respectively. However, reaction −R3 is the fastest process in the $CH_3OH + CH_3$ reaction system. The rate constant, k_{-R3} is 10 times greater than the rate constants of reactions R3 and R4 at 300 K. Therefore, the $CH_3O + CH_4 \rightarrow CH_3OH + CH_3$ reaction should be taken into account in modeling and experimental investigations of the $CH_3OH + CH_3$ reaction system. The methoxy radicals formed in reaction R3 are quickly converted back to the reactants in the reverse process −R3. It may explain why the methoxy radicals are not observed experimentally as products of the reaction of methyl radicals with methanol.

3.3. CH_3OH + OH Reaction System. The energy profile for the CH_3OH + OH reaction obtained at the G2 level shows only a small energy barrier for the hydroxymethyl formation, which implies a high value of the rate constant for the R6 reaction channel and a weak temperature dependence. This is in line with the results of measurements. The kinetic data evaluation of Tsang[3] and the recent experiments of Hess and Tully[27] for the CH_3OH + OH reaction suggest a description of the kinetics by a three-parameter expression of the type $AT^n \exp(-E/T)$, with a negative exponential parameter, E, which is usually observed for reactions proceeding with the formation of intermediate complexes. A similar mechanism was suggested by theoretical considerations for H-abstraction from methanol by halogen atoms, F, Cl, and Br.[32] A hydrogen bonding molecular complex, MC6, has been found for the hydroxymethyl reaction channel so that the rate constant calculation for this reaction channel should be performed on the basis of eq 3. However, contrary to reactions of methanol with chlorine and bromine atoms,[32] the energy barrier found for the reverse reaction is, at the G2 level, 22.7 kcal/mol higher than the energy barrier for the dissociation of MC6 toward the products. Therefore, at a given energy E, the density of states of the activated complex for the reaction MC6 → products is considerably greater compared to the density of states of TS6. The rate constant for the first elementary step, $k_{R6,TST}$ (from eq 1), corresponds to the rate constant for the hydroxymethyl formation channel when the simple, one-step mechanism of this channel is assumed, $CH_3OH + OH \rightarrow CH_2OH + H_2O$. The $k_{R6,TST}$ should be a very good approximation for the "exact" (for the two-step reaction mechanism) rate constant, k_{R6} (from eq 3)

$$\frac{k_{R6}}{k_{R6,TST}} = \frac{\int_{V_{ts}}^{\infty} dE \sum_{J=0}^{J_m}\sum_{K=0}^{K_m} W_{ts}(E,J,K)\frac{W_{ac}(E,J,K)}{W_{ts}(E,J,K)+W_{ac}(E,J,K)}\exp(-E/RT)}{\int_{V_{ts}}^{\infty} dE \sum_{J=0}^{J_m}\sum_{K=0}^{K_m} W_{ts}(E,J,K)\exp(-E/RT)} \approx 1 \quad (14)$$

because the microcanonical branching fraction in the upper integral is close to unity. A lowering of k_{R6} relative to its upper limit given by $k_{R6,TST}$ can be expected only at very high temperatures as the result of an increase of importance of the reverse process, MC6 → reactants. For comparison, both eqs 1 and 3 were used in the calculation of the rate constant for the hydroxymethyl reaction channel (R6).

The rate constant calculations corresponding to the methoxy reaction channel were performed on the basis of eq 1 using the transition state theory. As for the previously discussed reactions, CH_3OH with H and CH_3, the molecular parameters of reactants TS5, TS6, and MC6, derived at G2 level, were used in the rate constants calculation. Calculated rate constants k_{R5} and k_{R6}, as well as values of the overall rate constant k_{ov} and the branching fraction for hydroxymethyl formation, are given in Tables 8 and 9. The tunneling factor used in the calculation of k_{R5} was derived using the unsymmetrical Eckart potential[38] and the unscaled imaginary frequency of TS5 obtained at the MP2/6-311G** level. At any temperature of this study, the rate constant for the formation of the hydroxymethyl radical, k_{R6}, is significantly greater than that for the competing (R5) reaction channel. Values of $k_{R6,TST}$ derived on the basis of eq 1 are very close to the "exact" k_{R6} obtained from eq 3. The difference does not exceed 15% at the highest temperature studied (3000 K). At low temperatures (below 1000 K) there is practically no difference in values of the rate constants calculated for the complex, $CH_3OH + OH \leftrightarrow MC6 \rightarrow CH_2OH + H_2O$ (k_{R6}) and the one-step $CH_3OH + OH \rightarrow CH_2OH + H_2O$ ($k_{R6,TST}$) reaction mechanism. An increase of the importance of the reverse process (MC6 → reactants) at high temperatures is manifested by slightly lower values of k_{R6} compared to $k_{R6,TST}$. Calculated values of k_{R6} may be compared with recent results of the ab initio calculations of Pardo et al.[28] who studied this reaction channel (R6) at the MP4/6-311G**//MP2/6-31G* level. The values obtained in their calculation, i.e., $k_{R6} = 4.1 \times 10^{-13}$, 1.4×10^{-12}, and 2.9×10^{-12} cm^3 $molecule^{-1}$ s^{-1} at 300, 600, and 800 K, are however considerably lower than those derived in this study, i.e., 7.1×10^{-13}, 3.5×10^{-12}, and 7.3×10^{-12} cm^3 $molecule^{-1}$ s^{-1}, respectively. Despite the high tunneling factors used in their calculation, the results of Pardo et al.[28] are also lower than the most credible experimental results of Hess and Tully.[27] It is a consequence of the 5.5 kcal/mol higher energy barrier which was found by Pardo et al.[28] for the hydroxymethyl reaction channel. The values of k_{ov} obtained in this study are in very good agreement with the experimental measurements below 600 K. Our calculated value, $k_{ov} = 7.6 \times 10^{-13}$ cm^3 $molecule^{-1}$ s^{-1}, at 300 K is in line with $(0.8-1.1) \times 10^{-12}$ cm^3 $molecule^{-1}$ s^{-1} from measurements of Meier et al.,[23,24] Hägele et al.,[22] Ravishankara and Davis,[20] Overend and Paraskevopoulos,[21] and Campbell et al.[19] The considerably smaller value of 9.6×10^{-14} cm^3 $molecule^{-1}$ s^{-1} of Osif et al.[18] is obviously in error. At higher temperatures, our results overestimate the value of k_{ov} by a factor of 2 in comparison with the results of Hess and Tully[27] and those recommended by Tsang.[3] The temperature

TABLE 8: Calculated Rate Constants for Formation of Methoxy, k_{R5}, and Hydroxymethyl, k_{R6}, Radicals for $CH_3OH + OH$ Reaction System and for the Inverse Reactions, k_{-R5} and k_{-R6}

T (K)	$k_{R5,TST}$ (cm^3 $molec^{-1}$ s^{-1})	k_{R5}	k_{R5} (cm^3 $molec^{-1}$ s^{-1})	K_5[a]	k_{-R5} (cm^3 $molec^{-1}$ s^{-1})	k_{R6}[b] (cm^3 $molec^{-1}$ s^{-1})	$k_{R6}/k_{R6,TST}$	k_6[c]	k_{-R6} (cm^3 $molec^{-1}$ s^{-1})
300	1.91×10^{-15}	27.52	5.25×10^{-14}	8.31×10^{9}	6.32×10^{-24}	7.05×10^{-13}	1.00	2.28×10^{16}	3.09×10^{-29}
350	4.77×10^{-15}	14.20	6.77×10^{-14}	3.73×10^{8}	1.81×10^{-22}	9.90×10^{-13}	1.00	1.31×10^{14}	7.54×10^{-27}
400	9.82×10^{-15}	8.84	8.68×10^{-14}	3.64×10^{7}	2.39×10^{-21}	1.34×10^{-12}	1.00	2.78×10^{12}	4.81×10^{-25}
450	1.78×10^{-14}	6.21	1.10×10^{-13}	5.93×10^{6}	1.86×10^{-20}	1.75×10^{-12}	1.00	1.39×10^{11}	1.26×10^{-23}
500	2.94×10^{-14}	4.74	1.39×10^{-13}	1.39×10^{6}	1.00×10^{-19}	2.24×10^{-12}	1.00	1.28×10^{10}	1.75×10^{-22}
550	4.53×10^{-14}	3.84	1.74×10^{-13}	4.22×10^{5}	4.12×10^{-19}	2.82×10^{-12}	1.00	1.82×10^{9}	4.71×10^{-21}
600	6.63×10^{-14}	3.24	2.15×10^{-13}	1.56×10^{5}	1.37×10^{-18}	3.49×10^{-12}	1.00	3.58×10^{8}	1.55×10^{-21}
650	9.31×10^{-14}	2.82	2.63×10^{-13}	6.72×10^{4}	3.91×10^{-18}	4.26×10^{-12}	1.00	9.06×10^{7}	9.75×10^{-20}
700	1.27×10^{-13}	2.52	3.19×10^{-13}	3.26×10^{4}	9.79×10^{-18}	5.15×10^{-12}	1.00	2.79×10^{7}	1.84×10^{-19}
750	1.68×10^{-13}	2.29	3.84×10^{-13}	1.74×10^{4}	2.21×10^{-17}	6.16×10^{-12}	1.00	1.01×10^{7}	6.12×10^{-19}
800	2.17×10^{-13}	2.11	4.58×10^{-13}	9.99×10^{3}	4.58×10^{-17}	7.30×10^{-12}	1.00	4.13×10^{6}	1.77×10^{-18}
850	2.75×10^{-13}	1.97	5.43×10^{-13}	6.13×10^{3}	8.86×10^{-17}	8.58×10^{-12}	1.00	1.88×10^{6}	4.57×10^{-18}
900	3.43×10^{-13}	1.86	6.38×10^{-13}	3.96×10^{3}	1.61×10^{-16}	1.00×10^{-11}	1.00	9.30×10^{5}	1.07×10^{-17}
950	4.22×10^{-13}	1.77	7.46×10^{-13}	2.68×10^{3}	2.78×10^{-16}	1.16×10^{-11}	1.00	4.96×10^{5}	2.33×10^{-17}
1000	5.13×10^{-13}	1.69	8.66×10^{-13}	1.88×10^{3}	4.60×10^{-16}	1.33×10^{-11}	1.00	2.82×10^{5}	4.72×10^{-17}
1500	2.24×10^{-12}	1.32	2.95×10^{-12}	1.94×10^{2}	1.52×10^{-14}	4.06×10^{-11}	0.98	7.54×10^{3}	5.38×10^{-15}
2000	6.02×10^{-12}	1.19	7.16×10^{-12}	5.98×10^{1}	1.20×10^{-13}	8.81×10^{-11}	0.95	1.18×10^{3}	7.49×10^{-14}
3000	2.25×10^{-11}	1.10	2.47×10^{-11}	1.74×10^{1}	1.42×10^{-12}	2.46×10^{-10}	0.85	1.72×10^{2}	1.43×10^{-12}

[a] The equilibrium constant for $CH_3OH + OH \leftrightarrow CH_3O + H_2O$. [b] From eq 3. [c] The equilibrium constant for $CH_3OH + OH \leftrightarrow CH_2OH + H_2O$.

TABLE 9: Values of Calculated and Experimental Overall Rate Constants, $k_{ov,calc}$ and $k_{ov,exp}$, and Theoretical Branching Ratio of the Hydroxymethyl Reaction Channel, $\Gamma(CH_2OH)$ for $CH_3OH + OH$ Reaction[a]

T (K)	$k_{ov,calc}$ (cm^3 $molec^{-1}$ s^{-1})	$k_{ov,exp}$[b] (cm^3 $molec^{-1}$ s^{-1})		$\Gamma(CH_2OH)$ calcd	$\Gamma(CH_2OH)$ exptl
300	7.6×10^{-13}	1.0×10^{-12}	$(0.8-1.0) \times 10^{-12}$	0.93	0.89×0.03[22]
350	1.1×10^{-12}	1.2×10^{-12}	$(0.9-1.4) \times 10^{-12}$	0.94	
400	1.4×10^{-12}	1.4×10^{-12}	$(1.2-1.8) \times 10^{-12}$	0.94	0.78×0.07[22]
450	1.9×10^{-12}	1.7×10^{-12}	$(1.5-2.2) \times 10^{-12}$	0.94	
500	2.4×10^{-12}	2.0×10^{-12}	$(1.8-2.6) \times 10^{-12}$	0.94	0.85×0.05[c]
550	3.0×10^{-12}	2.3×10^{-12}	$(2.1-3.0) \times 10^{-12}$	0.94	
600	3.7×10^{-12}	2.6×10^{-12}	$(2.4-3.3) \times 10^{-12}$	0.94	0.71[d]
650	4.5×10^{-12}	3.0×10^{-12}	$(2.7-3.6) \times 10^{-12}$	0.94	
700	5.5×10^{-12}	3.5×10^{-12}	$(2.9-3.9) \times 10^{-12}$	0.94	
750	6.6×10^{-12}	3.9×10^{-12}	$(3.1-4.4) \times 10^{-12}$	0.94	
800	7.8×10^{-12}	4.5×10^{-12}	$(3.3-5.1) \times 10^{-12}$	0.94	
850	9.1×10^{-12}	5.0×10^{-12}	$(4.7-5.8) \times 10^{-12}$	0.94	
900	1.1×10^{-11}	5.6×10^{-12}	5.0×10^{-12}	0.94	
950	1.2×10^{-11}	6.3×10^{-12}	5.2×10^{-12}	0.94	
1000	1.4×10^{-11}	6.9×10^{-12}	8.3×10^{-12}	0.94	
1500	4.4×10^{-11}	1.7×10^{-11}	1.8×10^{-11}	0.93	
2000	9.5×10^{-11}	3.2×10^{-11}	2.6×10^{-11}	0.92	
3000	2.7×10^{-10}	8.1×10^{-11}		0.91	

[a] $k_{ov} = k_{R5} + k_{R6}$; $\Gamma(CH_2OH) = k_{R6}/k_{ov}$. [b] From Tsang equation[3]: $(1.1 \times 10^{-19})T^{2.53} \exp(483/T)$ (left column) and range of experimental results from refs 7 and 18−27 (right column). [c] From ref 11 at 482 K. [d] From ref 11 at 612 K.

dependence of the rate constants derived in this study can be expressed by the three-parameter nonlinear fits

$$k_{R5} = (7.6 \times 10^{-15})(T/300)^{3.4} \times \exp(575/T)\ \mathrm{cm^3\ molecule^{-1}\ s^{-1}} \quad (15)$$

$$k_{R6} = (3.5 \times 10^{-13})(T/300)^{2.8} \times \exp(210/T)\ \mathrm{cm^3\ molecule^{-1}\ s^{-1}} \quad (16)$$

with a small negative exponential parameter, E, for both reaction channels. It agrees with the results of Tsang[3] and Hess and Tully[27] who derived similar three-parameter equations for the temperature dependence of k_{R6}. Because of the small energy barrier for both reaction channels, the temperature dependence of the rate constants is mainly related to entropic contributions and therefore leads to non-Arrhenius behavior of k_{R5} and k_{R6}. The calculated branching ratios indicate a dominance of the R6 reaction channel. This is in line with the experimental results. However, some increase with temperature of the importance of the methoxy reaction channel has been reported.[11,22,27] It is interesting to note that the theoretical branching ratios are indeed temperature independent, and they indicate that at temperature below 1500 K about 94% of methanol is converted to hydroxymethyl radicals.

An Arrhenius plot of the calculated overall rate constant, $k_{ov} = k_{R5} + k_{R6}$, is shown in Figure 8, along with results of available experimental investigations and kinetic data evaluations. In the low-temperature range (below 600 K), our k_{ov} agrees well with experiments. At high temperatures, some measurements show considerable scatter. Results of Bowman[17] and Westbrook and Dryer[1b] are clearly incompatible with the experiments of Vandooren and Van Tiggelen.[7] The temperature dependence of the rate constant given by Tsang's equation[3] was derived taking into account results of Vandooren and Van Tiggelen,[7] which also nicely matches a high-temperature extrapolation of the results of Hess and Tully.[27] The kinetic data evaluation made by Warnatz[9] predicts significantly lower values of the rate constant k_{ov} in this temperature range. However, his analysis based on the two-parameter Arrhenius-type fit seems to be less realistic compared with Tsang's recommendation. The temperature dependence of our calculated k_{ov} is close to that predicted by Tsang which is manifested by nearly parallel curves in the high-temperature range. However, our calculated values of k_{ov} are slightly higher than those obtained from Tsang's equation.

Our derived overall rate constant k_{ov} is, at room temperature, a few orders of magnitude higher than the values discussed previously for the reactions of methanol with hydrogen and methyl radicals. This can be explained by the greater exothermicity of the reaction $CH_3OH + OH$ together with the small barrier heights found by the calculation. On the other hand, this reaction proceeds slower than the almost thermoneutral reaction of methanol with chlorine atoms.[12] The explanation of this peculiarity is related to the $CH_3OH + Cl$ reaction mechanism. As was shown in our preceding paper,[32] the reaction of methanol with chlorine atoms proceeds in the first elementary step with the formation of a weak intermediate complex, and the total energies of all stationary points (products, transition states, and molecular complexes) for the dominant hydroxymethyl channel

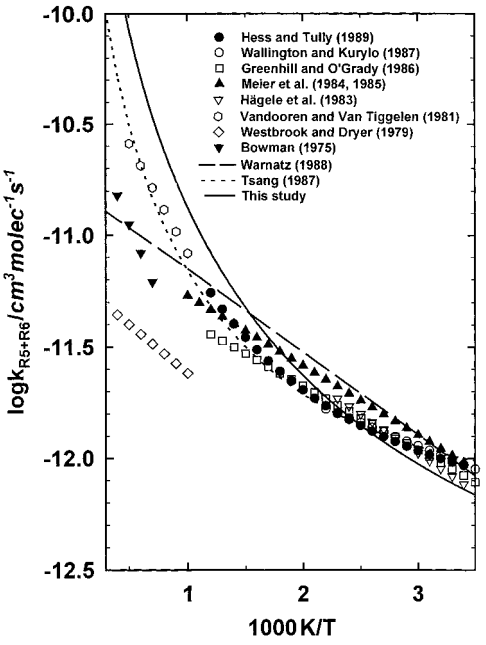

Figure 8. Arrhenius plot for the $CH_3OH + OH$ reaction comparing kinetic measurements (symbols) with data evaluations (lines) in the functional form $AT^n \exp(-E/T)$ of Hess and Tully[27] (294−866 K, R5 + R6: $A = 5.89 \times 10^{-20}$, $n = 0$, $E = -444$); Wallington and Kurylo[26] (240−440 K, R5 + R6: 4.8×10^{-12}, 0, 480); Greenhill and O'Grady[25] (260−803 K, R5 + R6: 8.0×10^{-12}, 0, 664); Meier et al.[23] (300−1000 K, R5 + R6: 1.1×10^{-11}, 0, 718); Hägele et al.[22] (295−420 K, R5 + R6: 1.2×10^{-11}, 0, 810); Vandooren and Van Tiggelen[7] (1000−2000 K, R5 + R6: 8.0×10^{-11}, 0, 2266); Westbrook and Dryer[1c] (1000−2180 K, R5 + R6: 6.6×10^{-12}, 0, 1006); Bowman[17] (1545−2180 K, R5 + R6: 5.0×10^{-11}, 0, 2999); Warnatz[9] (300−2000 K, R5 + R6: 1.7×10^{-11}, 0, 854); Tsang[3] (300−2000 K, R5 + R6: 1.1×10^{-19}, 2.53, −483); this study eqs 15 and 16.

are located below the energy level of reactants. Therefore, unimolecular processes play a very important role in the reaction kinetics and determine the reaction rate.

The calculated potential energy surface allows also the evaluation of the rate constants associated with the reverse reactions $CH_3O + H_2O \rightarrow CH_3OH + OH$ (−R5) and $CH_2OH + H_2O \rightarrow CH_3OH + OH$ (−R6) by using the equilibrium constants obtained theoretically from molecular parameters of reactants and products. The rate constants, k_{-R5} and k_{-R6}, obtained by this way are given in Table 8 and can be expressed as

$$k_{-R5} = (1.5 \times 10^{-15})(T/300)^{3.8} \times \exp(-5780/T)\ \text{cm}^3\ \text{molecule}^{-1}\ \text{s}^{-1} \quad (17)$$

$$k_{-R6} = (4.2 \times 10^{-14})(T/300)^{3.0} \times \exp(-10440/T)\ \text{cm}^3\ \text{molecule}^{-1}\ \text{s}^{-1} \quad (18)$$

Both reverse reactions are strongly endothermic and are slow processes with the rate constants at 300 K $k_{-R5} = 6.4 \times 10^{-24}$ cm^3 molecule^{-1} s^{-1} and $k_{-R6} = 3.3 \times 10^{-29}$ cm^3 molecule^{-1} s^{-1}. Therefore, those reactions do not play any role in the subsequent fate of the methoxy and hydroxymethyl radicals in the $CH_3OH + OH$ reaction system.

3.4. Comparison of Results Obtained at Different Levels of Theory. The calculated rate constants are mainly determined by the height of the energy barriers. The kinetics of the reactions under investigation presented in this work was based on the molecular parameters obtained in the G2 approach which is known to provide a correct description of the reaction energetics,

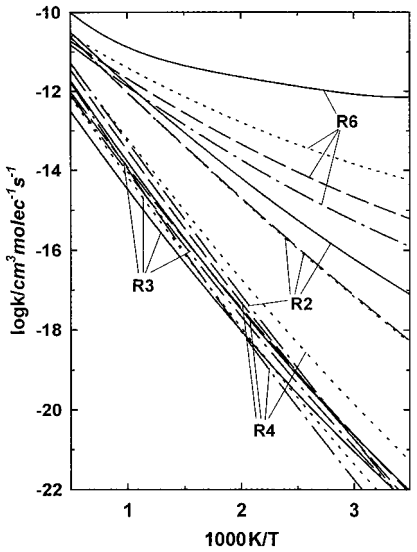

Figure 9. Rate constants for the reaction channels R2, R3, R4, and R6 calculated using different molecular parameters sets: (− · −) results of calculation with MP2/6-31G* energy barriers and vibrational frequencies scaled by 0.94; (···) MP2/6-311G** energy barriers and vibrational frequencies scaled by 0.94; (− − −) MP4/6-311G**//MP2/6-311G** energy barriers and vibrational frequencies as above; (—) G2 energy barriers and the SCF/6-31G* vibrational frequencies scaled by 0.8929.

However, it is interesting to make a comparison of the rate constants calculated using molecular parameters calculated by other ab initio approaches. The rate constants for reactions 2−6 as a function of temperature, based on the molecular parameters obtained at different levels of theory, are shown in Figure 9.

The height of the energy barrier for the reaction channel R6 depends strongly on the method of calculation. This is reflected by the scattered values of the calculated rate constants, $k_{R6,TST}$, at room temperature, 3.2×10^{-16}, 1.2×10^{-14}, 1.5×10^{-15} and 7.0×10^{-13} cm^3 molecule^{-1} s^{-1}, obtained at the MP2/6-31G*, MP2/6-311G**, MP4/6-311G**, and G2 levels, respectively. The significant dependence of the calculated rate constants on the molecular parameters used is also observed for the reaction R2. Values of $k_{R2,TST}$, 1.7×10^{-22}, 1.6×10^{-18}, 1.7×10^{-18} and 1.4×10^{-17} cm^3 molecule^{-1} s^{-1}, have been found at 300 K, for the respective levels of theory described above. On the other hand, the rate constants for the $CH_3OH + CH_3$ reaction system are considerably less sensitive to the choice of the ab initio data. The scattering of the values of the rate constants for both reaction channels, $k_{R3,TST}$ and $k_{R4,TST}$ does not exceed 1 order of magnitude. It is a result of the very close heights of the energy barriers derived at each level of theory for reaction channels, R3 and R4.

The zero-point energies calculated either using MP2 vibrational frequencies scaled by 0.94 or scaled SCF frequencies as in the G2 approach are very close. However, the use of nonscaled MP2 frequencies leads also to very close rate constant values (less than 10% different) in the temperature range studied. Considerably higher change of the rate constant is observed when the MP2 frequencies are replaced by their scaled SCF counterparts. Results of calculation performed for R2 and R6 reaction channels show that using scaled SCF frequencies yields rate constant values 2 times (R2) and 3 times (R6) higher at room temperature.

4. Conclusions

Ab initio calculations at different levels of theory and with different basis sets were performed for the $CH_3OH + H$, CH_3-

$OH + CH_3$ and $CH_3OH + OH$ reaction systems. Derived molecular properties of the stationary points of the potential energy surface were used for the description of the mechanism and the kinetics of the reactions under investigation. Results of calculation show that H-abstraction from methanol by H, CH_3, and OH proceeds by a simple one-step mechanism for methoxy formation reaction channels. The mechanism of the hydroxymethyl formation channel for the $CH_3OH + OH$ reaction system is more complex, but the rate constant is also determined by the energy barrier of the first elementary step. The reaction rates of all reactions studied are then only highly dependent on the molecular properties of their respective transition states. This behavior is different from the one of the reactions of methanol with halogen atoms (F, Cl, and Br) which has been shown to proceed via formation of weakly bonded intermediate complexes in the first elementary step; these complexes playing an important role in the reaction kinetics.[32]

The best agreement between calculated and experimental reaction enthalpies was reached using G2 calculations. However, the simplified procedures of the G2MP2, G2MP3, and G1 methods yield also reaction energies very close to the "exact" G2 values; this confirms that the G2MP2 method is the most economic way for improvement of reaction energetics. The calculated barrier heights (obtained at G2 level) are very different from each other for the reactions under investigation in this work. The heights of the energy barriers of the $CH_3OH + H$ and $CH_3OH + OH$ systems indicate the dominance of the hydroxymethyl radicals reaction channel. In the case of $CH_3OH + CH_3$ reaction system, the calculated energy barriers for the competing reaction channels, (R3) and (R4), depend on the level of calculation. However, values of the energy barriers for both reaction channels are close to each other and their difference does not exceed 1.5 kcal/mol at any level of theory. The height of the energy barrier is the major parameter which determines the reaction rate. Heights of the energy barriers obtained in G2 calculations for the respective reaction channels can be ordered as $V_{R6} < V_{R5} < V_{R2} < V_{R3} \approx V_{R4} \approx V_{R1}$. Some rationalization of the H, CH_3, and OH reactivities toward methanol has been made in terms of polar effects.

Using the conventional transition state theory, the calculated values of the rate constants are in very good agreement with available experimental results and allow a description of the kinetics of the reactions under investigation with a precision at least not worse than the one given by various kinetic data evaluations. An excellent agreement between theoretical and experimental values of the overall rate constant has been reached for the $CH_3OH + CH_3$ reaction, in a wide range of temperatures. Values obtained for the overall rate constant of the $CH_3OH + OH$ system seem to be overestimated at high temperatures but reproduce very well the results of measurements in the low-temperature (below 800 K) range. This is the contrary to the $CH_3OH + H$ reaction.

For $CH_3OH + H$ and $CH_3OH + OH$ reactions, values of the calculated branching ratios indicate a distinct dominance of the hydroxymethyl-forming reaction channel at any temperature studied. The same is true at higher temperatures for the $CH_3OH + CH_3$ reaction system. This is in line with the results of experimental investigations which show the methoxy-forming reaction channel to be of minor importance.

Acknowledgment. This work has been performed under the auspices of European Contract 'Copernicus' CIPA-CT93-0163 "Chemical Kinetic Studies of Combustion related to Atmospheric Pollution". We also wish to thank the I.D.R.I.S. Computing Center in Orsay (CNRS—France) for CPU time facilities. Part of the numerical calculations was carried out in the Wroclaw Networking and Supercomputing Center (Poland).

References and Notes

(1) (a) Eyzat, P. *Rev. Assoc. Fr. Tech. Pet.* **1975**, *230*, 31. (b) Aronowitz, D.; Naegell, D. W.; Glassman, I. *J. Phys. Chem.* **1977**, *81*, 2555. (c) Westbrook, C. K.; Dryer, F. L. *Combust. Flame* **1980**, *37*, 171. (d) Norton, T. S.; Dryer, F. L. *Int. J. Chem. Kinet.* **1990**, *22*, 219.

(2) (a) Dóbé, S.; Bérces, T.; Turányi, T.; Márta, F.; Grussdorf, J.; Temps, F.; Wagner, H. Gg. *J. Phys. Chem.* **1996**, *100*, 19864. (b) Johnson, R. D., III; Hudgens, J. W. *J. Phys. Chem.* **1996**, *100*, 19874. (c) Dertinger, S.; Geers, A.; Kappert, J.; Wiebrecht, J. *Faraday Discuss. R. Soc.* **1995**, *102*, 31.

(3) Tsang, W. *J. Phys. Chem. Ref. Data* **1987**, *16*, 471.

(4) Grotheer, H. H.; Kelm, S.; Driver, H. S. T.; Hutcheon, R. J.; Lockett, R. D.; Robertson, G. N. *Ber. Bunsen-Ges. Phys. Chem.* **1992**, *96*, 1360.

(5) Hoyermann, K.; Sievert, R.; Wagner, H. Gg. *Ber. Bunsen-Ges. Phys. Chem.* **1981**, *85*, 149.

(6) Meagher, J. F.; Kim, P.; Lee, J. H.; Timmons, R. B. *J. Phys. Chem.* **1974**, *78*, 2650.

(7) Vandooren, J.; Van Tiggelen, P. J. *Experimental Investigation of Methanol Oxidation in Flames: Mechanisms and Rate Constants of Elementary Steps*; Symp. Combust. 18; Combustion Institute: Pittsburgh, 1981; p 473.

(8) Aders, W. K. *Reactions of H-Atoms with Alcohols*; Weinberg, F., Ed.; Combustion Institute, European Symposium; Academic Press: London **1973**, *1*, 19.

(9) Warnatz, J. *Rate Coefficients in the C/H/O System Combustion Chemistry*; Gardiner, W. C., Jr., Ed.; Springer-Verlag: New York, 1984; p 197.

(10) Spindler, K.; Wagner, H. Gg. *Ber. Bunsen-Ges. Phys. Chem.* **1983**, *86*, 2.

(11) Dóbé, S.; Bérces, T.; Temps, F.; Wagner, H. Gg.; Ziemer, H. In *Proceedings of the 25th Symposium (International) on Combustion*; Combustion Institute: Pittsburgh, 1994; p 775.

(12) Dóbé, S.; Otting, M.; Temps, F.; Wagner, H. Gg.; Ziemer, H. *Ber. Bunsen-Ges. Phys. Chem.* **1993**, *97*, 877.

(13) Lendvay, G.; Bérces, T.; Márta, F. *J. Phys. Chem. A* **1997**, *101*, 1588.

(14) Kerr, J. A.; Personage, M. J. *Evaluated Kinetic Data on Gas-Phase Hydrogen Transfer Reactions of Methyl Radicals*; Butterworth: London, 1976; p 95.

(15) (a) Campion, A.; Williams, F. *J. Am. Chem. Soc.* **1972**, *94*, 7633. (b) Hudson, R. L.; Shiotani, M.; Williams, F. *Chem. Phys. Lett.* **1977**, *48*, 193. (c) Doba, T.; Ingold, K. U.; Siebrand, W.; Wildman, T. A. *Faraday Discuss. Chem. Soc.* **1984**, *78*, 175. (d) Doba, T.; Ingold, K. U.; Siebrand, W.; Wildman, T. A. *J. Phys. Chem.* **1984**, *88*, 3165.

(16) Tachikawa, H.; Hokari, N.; Yoshida, H. *J. Phys. Chem.* **1993**, *97*, 10035.

(17) Bowman, C. T. *Combust. Flame* **1975**, *25*, 343.

(18) Osif, T. L.; Simonaitis, R.; Heicklen, J. *J. Photochem.* **1975**, *4*, 233.

(19) Campbell, I. M.; McLaughlin, D. F.; Handy, B. *J. Chem. Phys. Lett.* **1976**, *39*, 362.

(20) Ravishankara, A. R.; Davis, D. D. *J. Phys. Chem.* **1978**, *82*, 2852.

(21) Overend, R.; Paraskevopoulos, G. *J. Phys. Chem.* **1978**, *82*, 1329.

(22) Hägele, J.; Lorenz, K.; Rhasa, D.; Zellner, R. *Ber. Bunsen-Ges. Phys. Chem.* **1983**, *87*, 1023.

(23) Meier, V.; Grotheer, H. H.; Just, T. *Chem. Phys. Lett.* **1984**, *106*, 97.

(24) Meier, V.; Grotheer, H. H.; Rickert, G.; Just, T. *Ber. Bunsen-Ges. Phys. Chem.* **1985**, *89*, 325.

(25) Greenhill, P. G.; O'Grady, V. O. *Aust. J. Chem.* **1986**, *39*, 1775.

(26) Wallington, T. J.; Kurylo, M. J. *Int. J. Chem. Kinet.* **1987**, *19*, 1015.

(27) Hess, W. P.; Tully, F. P. *J. Phys. Chem.* **1989**, *93*, 1944.

(28) Pardo, L.; Banfelder, J. R.; Osman, R. *J. Am. Chem. Soc.* **1992**, *114*, 2382.

(29) Frisch, M. J.; Trucks, G. W.; Schlegel, H. B.; Gill, P. M. W.; Johnson, B. G.; Wong, M. W.; Foresman, J. B.; Robb, M. A.; Head-Gordon, M.; Replogle, E. S.; Gomperts, R.; Andres, J. L.; Raghavachari, K.; Binkley, J. S.; Gonzalez, C.; Martin, R. L.; Fox D. J.; Defrees, D. J.; Baker, J.; Stewart, J. P.; Pople, J. A. Gausssian Inc.: Pittsburgh, PA, 1993. Gaussian 92/DFT, revision F. 2; Frisch, M. J.; Trucks, G. W.; Schlegel, H. B.; Gill, P. M. W.; Johnson, B. G.; Robb, M. A.; Cheeseman, J. R.; Keith, T.; Petersson, G. A.; Montgomery, J. A.; Al-Laham, M. A.; Zakrzewski, V. G.; Ortiz, J. V.; Foresman, J. B.; Cioslowski, J.; Stefanov, B. B.; Nanayakkara, A.; Challacombe, M.; Peng, C. Y.; Ayala, P. Y.; Chen, W.; Wong, M. W.; Andres, J. L.; Replogle, E. S.; Gomperts, R.; Martin, R. L.; Fox, D. J.; Binkley, J. S.; Defrees, D. J.; Baker, J.; Stewart, J. P.; Head-Gordon, M.; Gonzalez, C.; Pople, J. A. Gaussian 94, revision D. 3; Gausssian Inc.: Pittsburgh, PA, 1995.

(30) Hehre, W. J.; Radom, L.; Schleyer, P.v. R.; Pople, J. A. *Ab Initio Molecular Orbital Theory*; Wiley: New York, 1986.

(31) Møller, C.; Plesset, M. S. *Phys. Rev.* **1934**, *46*, 618.

(32) Jodkowski, J. T.; Rayez, M. T.; Rayez, J. C.; Bérces, T.; Dóbé, S. *J. Phys. Chem. A*, **1998**, *102*, 9219; *J. Phys. Chem. A*, **1998**, *102*, 9230.

(33) (a) Pople, J. A.; Head-Gordon, M.; Raghavachari, K.; Curtiss, L. A. *J. Chem. Phys*. **1989**, *90*, 5622. (b) Curtiss, L. A.; Jones, C.; Trucks, G. W.; Raghavachari, K.; Pople, J. A. *J. Chem. Phys.* **1990**, *93*, 2537. (c) Curtiss, L. A.; Raghavachari, K.; Trucks, G. W.; Pople, J. A. *J. Chem. Phys.* **1991**, *94*, 7221. (d) Curtiss, L. A.; Raghavachari, K.; Pople, J. A. *J. Chem. Phys.* **1993**, *98*, 1293.

(34) (a) Chase, N. W., Jr.; Davies, C. A.; Downey, J. R., Jr.; Frurip, D. J.; McDonald, R. A.; Syverud, A. N. *J. Phys. Chem. Ref. Data* **1995**, *14*, suppl. 1 (JANAF Thermochemical Tables, 3rd ed.). (b) Gluschko, V. P.; Gurvich, L. V.; Bergman, G. A.; Veyts, I. V.; Medvedeev, V. A.; Chachkuruzov, G. A.; Yungman, V. S. *Termodinamitcheskoe Svoistva Individualnych Vestchestv*; Nauka: Moscow, 1974. (c) Benedict, W. S.; Gailer, N.; Plyler, E. K. *J. Chem. Phys.* **1956**, *24*, 1139.

(35) (a) DeMore, W. B.; Sander, S. P.; Golden, D. M.; Hampson, R. F.; Kurylo, M. J.; Howard, C. J.; Ravishankara, A. R.; Kolb, C. E.; Molina, M. J. *Chemical Kinetics and Photochemical Data for Use in Stratospheric Modeling*, Evaluation No. 11; JPL Publ. 94-26; NASA Panel for Data Evaluation; Jet Propulsion Laboratory, California Institute of Technology: Pasadena, 1994; p 194.

(36) (a) Melius, C. F. In *Chemistry and Physics of Energetic Materials*; Bulusu, S. N., Ed.; Kluwer Academic Publishers: Dordrecht, The Netherlands, 1990. (b) Ho, P.; Melius, C. F. *J. Phys. Chem*. **1995**, *99*, 2166. (c) Allendorf, M. D.; Melius, C. F. *J. Phys. Chem*. **1993**, *97*, 720.

(37) (a) Benson, S. W. *Thermochemical Kinetics*; 2nd ed.; Wiley: New York, 1976. (b) Laidler, K. J. *Theories of Chemical Reaction Rates*; McGraw-Hill: New York, 1969.

(38) (a) Johnston, H. S.; Rapp, D. *J. Am. Chem. Soc.* **1961**, *83*, 1. (b) Johnston, H. S.; Heicklen, J. *J. Chem. Phys.* **1962**, *66*, 532. (c) Johnston, H. S. *Gas-Phase Reaction Rate Theory*; The Ronald Press Co.: New York, 1966.

(39) (a) Troe, J. *J. Chem. Phys.* **1981**, *75*, 226. (b) Troe, J. *J. Chem. Phys.* **1983**, *79*, 6017.

(40) (a) Forst, W.; Prášil, Z. *J. Chem. Phys.* **1969**, *51*, 3006. (b) Hoare, M. R. *J. Chem. Phys.* **1970**, *52*, 5695.